Ignition and Combustion Characteristics of Flammable Gas Mixtures over Hot Surfaces

Lea Duedahl Pedersen

Master's Thesis Project, June 2016
Thermal Energy and Process Engineering

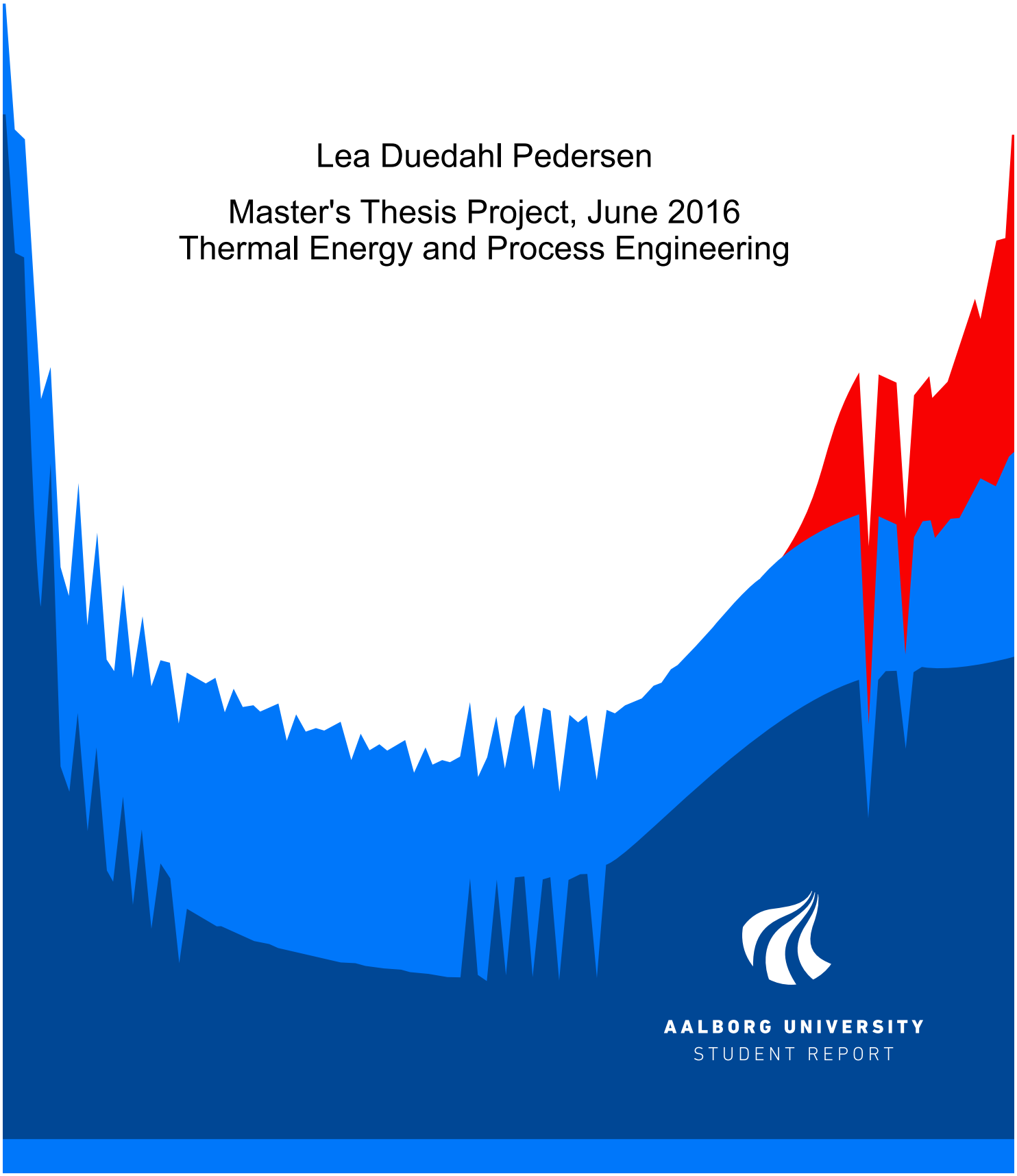

AALBORG UNIVERSITY
STUDENT REPORT

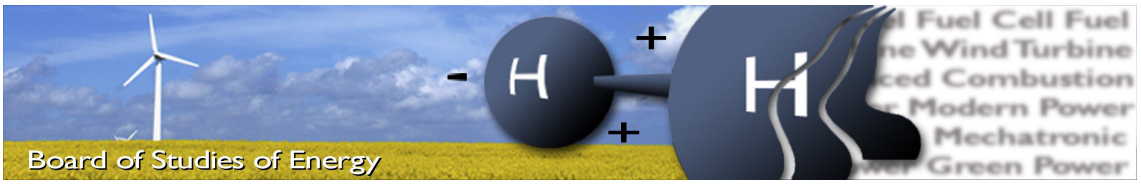

Title:	Ignition and combustion characteristics of flammable gas mixture over hot surfaces
Semester:	10^{th}, spring semester 2016
Semester theme:	Master's Thesis
Project period:	01.02.2016 to 01.06.2016
ECTS:	30
Supervisors:	Chungen Yin and Henrik Sørensen
Project group:	TEPE4-1002 / Lea Duedahl Pedersen

SYNOPSIS:
Ignition and combustion characteristics are investigated for flammable gas mixture passing over hot surfaces. Hot surfaces in gas turbines on offshore oil and gas facilities are estimated to introduce an unwanted risk of fire and explosion that can cause extensive damage and loss of human lives.
An extensive literature survey is conducted to gain an understanding of the mechanism involved in hot surface ignition, and how physical and chemical conditions affect it. State of the art review on modelling hot surface ignition and combustion inspired to develop a model procedure for dealing with flammable gas mixture over hot surfaces.
It is succeeded to develop and implementing a functional model in ANSYS CFX. Simulation results show a physical responses that correspond to trends experimentally determined in other studies. It is found that the hot surface ignition temperature (HSIT) increases with increased velocity and turbulence. The HSIT decreases with increase initial temperature. It was found that the HSIT decreases with increasing pressure, until some point, after which the HSIT increase again.
Based on the estimated risk, suggestion for practical requirements to a mitigation system are investigated. Mitigation measures such as cranking and adding diluent are suggested. Where cranking requires an extensive knowledge of the gas turbine flow profile, flammability limits with added diluents can be used independently of the specific gas turbine. No ignition is possible outside the flammability limits, making it a useful risk analysis criterion. Information on flammability limits with added diluent are determined by standardised tests making relevant data easier accessible. A procedure for including the effect of diluent in the CFD model are suggested.

Pages, total: 78
Appendixes: 2

Preface

This Master's Thesis was composed between February 1st and June 1st 2016 finalising a Master in Thermal Energy and Process Engineering at Aalborg University. The project aims to understand and model ignition and combustion characteristics of flammable gas passing over hot surfaces. It is of interest to understand hot surface ignition and combustion in order to avoid risk of ignition of flammable gas in gas turbines on offshore oil and gas facilities. Additional understanding of mitigation measures is aimed in order to propose a practical solution to the oil an gas industry.

The report presupposes a level of knowledge about fundamental combustion, Computational Fluid Dynamics (CFD) and gas turbine operation. Furthermore it is useful, but not strictly necessary, to possess knowledge about ANSYS CFX, which is used for modelling.

Thesis structure:
The content of this thesis cover three main areas, each presented in their own chapter.

- **Chapter 2** contain an extensive literature survey in order to understanding hot surface ignition. This includes understanding typical surface temperature that leads to ignition and how physical and chemical properties affect that temperature. Additionally a literature survey is conducted of academic and industrial modelling approaches determining the risk of hot surface ignition.
- **Chapter 3** present a developed CFD model of hot surface ignition and combustion. The modelling approach and important considerations handling ignition and combustion are presented in addition to simulation results of surface temperature leading to ignition.
- **Chapter 4** focus on mitigation measures and how to set up practical requirements to a mitigation system. Requirements are discussed in terms of applicability in the industry. A suggestion to an implementation procedure for including mitigation measure in the developed CFD is presented last.

Citation:
The report conforms to the scientific standard of citing the sources used throughout. The report follows the Harvard citation method, where sources are listed in the text as [Surname, year]. This citation refers to the bibliography at the end of the report, where books are listed with author, year, title, edition and publisher; Websites are listed with author, title, date and URL. The bibliography is in alphabetically order.

Figures, tables and equations are numbered according to chapter and order of appearance therein.

Nomenclature

Abbreviations

Abbreviation	Explanation
AIT	Auto Ignition Temperature
API	American Petroleum Institute
BVM	Burning Velocity Model
CEL	CFX Expression Language
CFD	Computational Fluid Dynamics
DDT	Deflagration-to-detonation
FLACS	FLame ACceleration Simulator
FZK	Forschungszentrum Karlsruhe
HP	High Pressure
HSE	Health and Safety Executive
HSIT	Hot Surface Ignition Temperature
HSL	Health and Safety Laboratory
IAEA	International Atomic Energy Agency
JIP	Joint Industry Project
KISMET	KIneticS Modelling EnvironmenT
LES	Large Eddy Simulation
LFL	Lower Flammability Limit
LRC	Lloyd's Register Consulting
MIE	Minimum Ignition Energy
PDF	Probability density function
PSA	Petroleum Safety Authority
TCF	Turbulent Flame Closure
UDF	User Defined Function
UNEP	United Nations Environmental Program
UT	University of Twente
UFL	Upper Flammability Limit
SI	Spark Ignition
SST	Shear Stress Transport

Symbol list

Symbol	Explanation	Unit
a	Temperature dependent coefficient	[–]
A	Pre-exponential factor	[s^{-1}]
α	Thermal diffusivity	[m^2/s]
b	Temperature dependent coefficient	[–]
B	Sink term constant	[kg/m^3 s]
β	Zeldovich number	[–]
c	Reaction progress variable	[–]
C	Stoichiometric coefficient for fuel	[–]
C	Courant number	[–]
C_p	Specific heat at constant pressure	[J/Kg K]
C_x	Constant	[s^{-1}]
D	Mass diffusivity	[m^2/s]
D	Stoichiometric coefficient for air	[–]
E_a	Activation energy	[J/mol]
E_n	Dimensionless activation energy $E_n = E_a/RT_\infty$	[–]
ε	Turbulent dissipation rate	[m^2/s^3]
f	Friction factor	[–]
δ_c	critical F-K parameter	[–]
δ_f	Laminar flame thickness	[m]
ΔH_c	Heat of combustion	[Kcal/mol]
I	Turbulence intensity	[–]
I_{gn}	Ignition parameter	[–]
k	Turbulent kinetic energy	[m^2/s^2]
k	Thermal conductivity	[W/m K]
L	Lower Flammability Limit	[vol%]
Le	Lewis number	[–]
m_f	Partial order with respect to fuel	[–]
m_o	Partial order with respect to oxidiser	[–]
M	Molar mass of gas mixture	[g/mol]
μ	Dynamic viscosity	[Pa · s]
n	Overall reaction order, $n = m_f + m_o$	[–]
n	Dimensions	[–]
ν	Kinematic viscosity	[m^2/s]
ω_c	Reaction source term	[Kg/m^3 s]
P	Probability	[–]
P	Pressure	[Pa]
ϕ	Equivalents ratio	[–]
Φ	Variable	[–]
Pr	Prandtl number	[–]
q	Rate of heat	[J/m^2 s]
Q	Heat of combustion	[J/mol]
r_f	Molar reaction rate	[mol/m^3 s]
r_f	Critical radius of hot pocket of burned gas	[m]
R	Ideal gas constant	[J/mol K]

Symbol	Explanation	Unit
$\tilde{R}$	Elapsed fraction of ignition delay time	[–]
Re	Reynolds number	[–]
ρ	Density	[kg/m^3]
S_c	Combustion source term	[–]
S_L	Laminar flame speed	[m/s]
S_T	Turbulent burning velocity	[m/s]
σ	Schmidt number	[–]
t	Time	[s]
Δt	Time step size	[s]
T	Temperature	[K]
T_{act}	Activation temperature	[K]
τ_{ign}	Ignition time delay	[μs]
u	Velocity	[m/s]
u'	RMS of the turbulent velocity fluctuations	[m/s]
U	Mean velocity	[m/s]
x	Directional component	[m]
X	Scalar dissipation rate	[–]
Δx	Length interval	[m]
X_F	Mole fraction of fuel	[mol/mol]
X_O	Mole fraction of oxidiser	[mol/mol]
Y_i	Species mass fraction	[–]
Z_i	Mean mixture fraction	[–]
Z_i''	Mixture fraction variance	[–]

Commonly used sub- and superscripts

Symbol	Explanation
b	Burnt
D	Hydraulic diameter
$knock$	Autoignition knock model
u	Unburnt
w	Wall
∞	Ambient
$-$	RANS averaged variable
$\sim$	Favre averaged variable

Table of contents

1 Introduction

One of the worst offshore oil and gas disaster in history was the Piper Alpha platform accidence in 1988. 167 out of 228 workers died during the accident and over 100 safety recommendations were initiated after a gas leak let to a series of explosions [The Guardian, 2013]. Accidents involving hydrocarbon leaks have the potential to be devastating. Hydrocarbon explosions and fires were the main cause of more than 70% of the accidents occurring on offshore installations on the UK Continental Shelf from 1980-2005 [Paik et al., 2011] [Det Norske Veritas, 2007]. It was at the same time estimated by PSA, Norway [2016] that hydrocarbon leaks accounted, together with serious well incidents, damage to supporting structures and marine systems, and ships on collision course, for more than 80 % of total major risk accidents offshore from 1996-2004 on the Norwegian Continental Shelf. Hydrocarbon leaks can be divided into three categories: gas leaks, liquid leaks and multi-phase leaks, where gas leaks have the highest explosion risk leading to the greatest potential of causing damage [PSA, Norway, 2016]. The damage a accident cause and the risk frequency make it relevant to investigate gas ignition and combustion further.

Accidents involving flammable gas are no new risks and several academic, public and private companies have long been working on understanding, quantifying and limiting the risk of explosions and fires. Empathises should be on preventing any fires and explosions, by removing source of ignition or avoiding any leaks, but as it is not always possible it is important to control, and when a tolerable risk criteria is exceeded, mitigate the gas mixture.

Several standards exist with the purpose of preventing, controlling and mitigating fire and explosions on offshore facilities. In the UK the Health and Safety Executive (HSE) has the UKOOA standards which have to be abided by all on the UK Continental Shelf. Similarly, applies the NORSOK Standard S-001 on the Norwegian Continental Shelf. The interest organisation American Petroleum Institute (API) has made the API RP2A standard and ISO/FDIS 13702 is yet another standard concentrating control and mitigation of fires and explosions on offshore production facilities [HSE - Offshore Division, 2013]. Some operators have in addition their own guidelines when it comes to protect against fires and explosions.

Lloyd's Register, on behalf of the Norwegian oil and gas association, concluded in 2014 that the industry today could not demonstrate a tolerable risk when it applies to ensure that gas turbines did not introduce an unacceptable risk of ignition [Lloyd's Register Consulting, 2015]. Gas turbines for electricity production or part of the process area run at high temperature and pressure increasing the risk of ignition in situations where flammable gas is introduced at the gas turbine inlet [PSA, Norway, 2016].

Due to the estimated risk associated with gas turbines during gas leaks a Joint Industry Project (JIP) was kicked-off in September 2015 managed by Lloyd's Register Consulting (LRC). Oil and gas operators Maersk Oil and Gas, Statoil and ConocoPhilips are partners in the JIP besides LRC. Academic contracted partners in the JIP include University of Twente (UT) in the Netherlands and an industrial Ph.D from Nanyang Technological University/Lloyd's Register Global Technology Centre in Singapore.

The overall objectives of the JIP are:

- to investigate gas turbine behaviour when the intake air is contaminated with flammable gas
- to understand the mechanism and likelihood of the flammable gas ignition within the gas turbine

Based on the probability of ignition the JIP will investigate and propose practical mitigation measures to limit the risk to an acceptable level [Lloyd's Register Consulting, 2015].

Understanding gas turbine operation and shutdown was one of the main activities in the JIP Phase 0 conducted in the autumn 2015. I took part of the JIP Phase 0 as an intern in LRC in Copenhagen. Typical physical property intervals and important time scales were established through extensive literature study and continual contact with gas turbine vendors, mainly GE Oil and Gas in Italy and the United States. It was concluded that the risk of ignition within gas turbines could not be disproved and that the highest risk of ignition is from hot surfaces especially during a fast shut down [Lloyd's Register Consulting, 2016a]. The big difference between gas turbine models, operation and shutdown procedures makes it impossible to make a general conclusion of the risk of ignition. In a JIP meeting with GE Oil and Gas representatives, GE Oil & Gas [2016] acknowledged that hot surface ignition inside gas turbines is a potential risk in case of a gas leak. The importance of the JIP was after Phase 0 clear and a Phase 1 scope is being drawn up and planned to kick off in August 2016.

1.1 Thesis problem statement

The purpose of this thesis is to:

- Gain an in depth knowledge of the ignition mechanism and how hot surface ignition and combustion can be determined and modelled
- Develop a CFD model demonstrating how hot surface ignition and combustion can be modelled. Compare the simulation results to expected physical responses and estimate the risk of hot surface ignition in gas turbines offshore
- Determine a practical solution towards utilising mitigation measures to suppress fire and explosions in gas turbines offshore

Each activity are covered in Chapter 2, 3 and 4, respectively.

2 Hot surface ignition

Relevant theory in order to understand the hot surface ignition mechanism are presented in Section 2.1.

Section 2.2 contains a state of the art literature review forming the basis for being able to develop a numerical model that can predict hot surface ignition.

2.1 Understanding the ignition mechanism

The ignition mechanism is important to understand in order to predict the risk of ignition. Predicting hot surface ignition is difficult as it is dependent on several physical and chemical properties. Some of the parameters influencing ignition are listed below [Smyth and Bryner, 1991]:

- Surface temperature, material and conditions
- Fuel/air mixture
- Initial gas temperature and pressure
- Fuel type
- Turbulence
- Residence time
  - Gas mixture velocity
  - Surface size

The effect of influencing parameters on ignition is covered in more details throughout this section.

2.1.1 Surface temperature, conditions and material

Analysing hot surface ignition is often described by the minimum surface temperature for ignition to be possible. The minimum temperature is called the hot surface ignition temperature (HSIT).

Due to the complexity of hot surface ignition, the HSIT has historically mainly been determined experimentally. Some interesting work done to understand HSIT, what parameters affect and to what degree, is the experimental work by Mullen II et al. [1948] and Smyth and Bryner [1991].

Mullen II et al. [1948] tested the effect of surface conditions by conducting experiments with polished and sandblasted rods. Mullen II et al. [1948] could not, within the limit of experimental error, measure any difference in the HSIT due to surface conditions.

However the surface material is shown by Smyth and Bryner [1991] to affect the HSIT. The measured temperatures as a function of surface material and fuel type are presented in Table 2.1.

	Nickel Foil	Stainless Steel Foil	Titanium Foil
Methane	1040 ± 10 °C	814 ± 8 °C	1038 ± 8 °C
Ethane	896 ± 18 °C	767 ± 3 °C	810 ± 34 °C
Propane	914 ± 4 °C	805 ± 4 °C	847 ± 8 °C

Table 2.1. Surface material effect on hot surface ignition temperature (HSIT) under stoichiometric conditions [Smyth and Bryner, 1991].

The HSIT of methane is more than 200°C higher with a surface of nickel relative to a surface of stainless steel. Similar tendencies are seen for ethane and propane. Mullen II et al. [1948] noted little difference between the HSIT for a Type 304 stainless steel and Nichrome V surfaces, but with a platinum surface the HSIT needed to be 917°C higher for ignition. The effect of surface material is merely concluded with no explanation by Mullen II et al. [1948] and Smyth and Bryner [1991]. The effect on HSIT could be due to interaction between gas and surface material or due to the heat transfer properties of the surface material, but no papers validating or rejecting these hypothesis have been found.

One of the main risks associated with hot surface ignition in gas turbines is estimated to be during fast shut down. If the gas turbine shuts down, causing the flow to decrease, faster than hot material cools below the HSIT the risk of hot surface ignition increases dramatically. The cooling profile of the hot surfaces is dependent on the amount and type of material.

2.1.2 Fuel/air mixture

Figure 2.1 shows the experimentally measured HSITs of ethylene/air as a function of different mixture compositions.

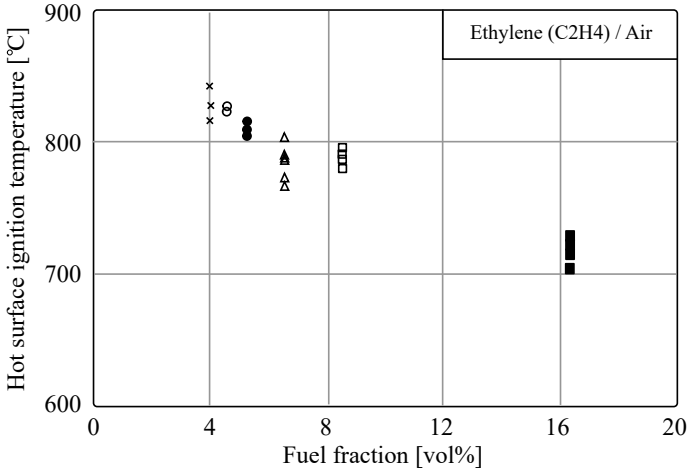

Figure 2.1. HSIT of Ethylene/air as a function of fuel/air mixture [Smyth and Bryner, 1991].

It is seen that as the fuel fraction increases, the HSIT decreases. Most fuels follow this tendency with lowest ignition temperature in the fuel rich region [Bounaceur et al., 2015]. Methane/air represents an exception having its lowest ignition temperature in the fuel lean range of 3-8 vol% [Kong et al., 1994] [Bounaceur et al., 2015]. Gas leaks occurring at offshore oil and gas facilities are most often of a size, so a mixture with air is in the fuel lean to stoichiometric range [Lloyd's Regiter Consulting, 2015].

An illustration of ignition regimes as a function of fuel fraction and temperature is presented in Figure 2.2.

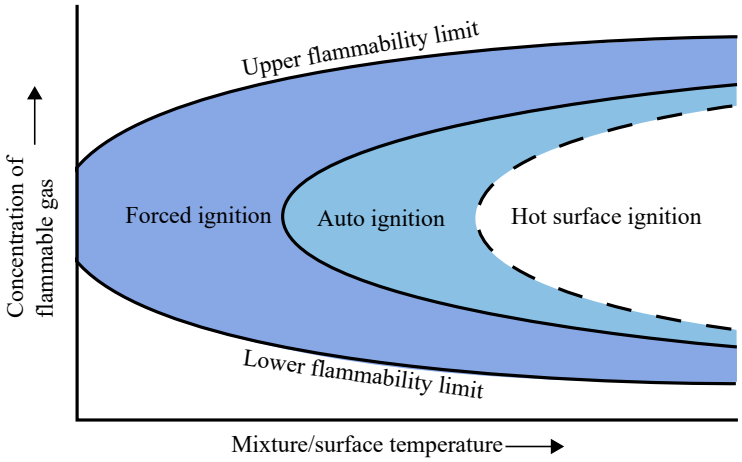

Figure 2.2. Flammability and ignition regimes as a function of temperature and fuel concentration. Inspired by Colwell and Reza [2005].

The Lower Flammability Limit (LFL) expresses the minimum amount of flammable gas needed for ignition to be possible and the Upper Flammability Limit (UFL) is an expression for the minimum amount of air (or more precisely oxygen) needed for ignition to be possible. Outside the flammability limits no ignition is possible. Within the flammability limits different ignition regimes exist: Forced ignition, autoignition and hot surface ignition.

For forced ignition, a source of ignition has to be present in order to start ignition. Autoignition expresses a regime where a mixture at high enough temperature can suddenly self ignite. The autoignition regime is sometimes also referred to as the spontaneous ignition regime. The temperature, at hot surface ignition, refers to the surface temperature and not the mixture temperature, as with the other two regimes. Studies have shown that the hot surface ignition temperature is at least 187°C higher than the autoignition temperature, which is the reason for the way of illustrating the regimes [American Petroleum Institude, 2003] [Colwell and Reza, 2005]. The hot surface temperature has to be higher for ignition due to the less ideal conditions e.g. presence of convective flow and a temperature gradient from the wall.

It can be seen from Figure 2.2 that the flammable range widens with increasing temperature. Details on the effect of temperature and pressure on hot surface ignition are described next.

2.1.3 Initial gas temperature and pressure

With an increase in initial temperature and pressure the flammable mixture range increases [Zabetakis, 1999] [Colwell and Reza, 2005].

White [1925] showed that the LFL is linearly dependent on temperature, with a drop of 6-8 % per 100°C, for hydrogen, methane, ethyl ether, carbon monoxide, acetylene and ethylene. This tendency is known as the White criteria or White's law [Zabetakis, 1999] [Kondo et al., 2011]. Vanderstraeten et al. [1997] showed by comparing experimental data that the LFL is not remarkably affected by changing the initial pressure between 1 and 10 bar. Similar conclusion was reached by Coward and Jones [1952] for a pressure range of 0.2 - 1 bar. The pressure affect on the flammability limits is shown for natural gas in Figure 2.3.

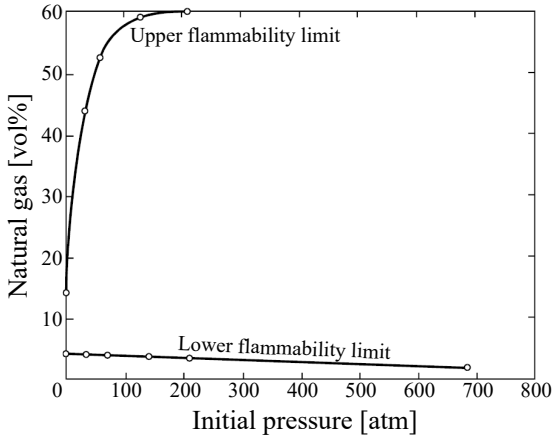

Figure 2.3. Upper and lower flammability limit of natural gas as a function of pressure [Zabetakis, 1999].

It can be seen from Figure 2.3 that the LFL decreases linearly with increasing pressure approximated by Equation (2.1).

$$\mathrm{LFL} = 4.9 - 0.71 \log \mathrm{P} \tag{2.1}$$

The pressure dependence is very small, so the constant LFL assumption in a smaller range of pressure is most often accepted.

The UFL is dependent on both temperature and pressure. Kondo et al. [2011] showed that the temperature coefficients determined from White's criterion on the LFL can reasonably be used to predict the UFL temperature dependence for simple combustible gases in the temperature range 5-100°C. Vanderstraeten et al. [1997] found that the UFL indeed is linearly dependent on temperature, but that the White's criterion could not be used at other than atmospheric pressure. The UFL is, according to Vanderstraeten et al. [1997], second order dependent on pressure and an expression of UFL should include both temperature and pressure dependency.

Experimental data by Mullen II et al. [1948] clearly state that increased initial temperature and pressure, decrease the hot surface temperature needed for ignition under the same

flow and fuel conditions. It should be noted that in the experimental set-up by Mullen II et al. [1948] only a pressure from 0-10 p.s.i.g (1-1.7 bar relative to vacuum) was tested. The effect of increased initial temperature and pressure on the autoignition temperature (AIT) was reported by Caron et al. [1999]. Similar to the HSIT, the AIT decreases with increasing temperature and pressure, as illustrated in the data from Caron et al. [1999] in Figure 2.4.

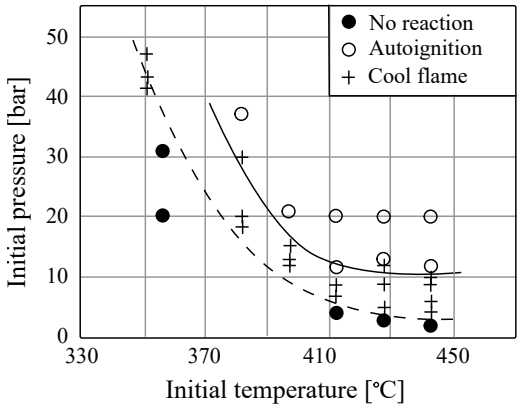

Figure 2.4. Autoignition as a function of initial temperature and pressure [Caron et al., 1999].

2.1.4 Fuel type

The more molecular compact fuel, the higher the AIT and HSIT [Fire Protection Association, 2014]. The effect of fuel type and molecular structure on AIT are illustrated in Figure 2.5.

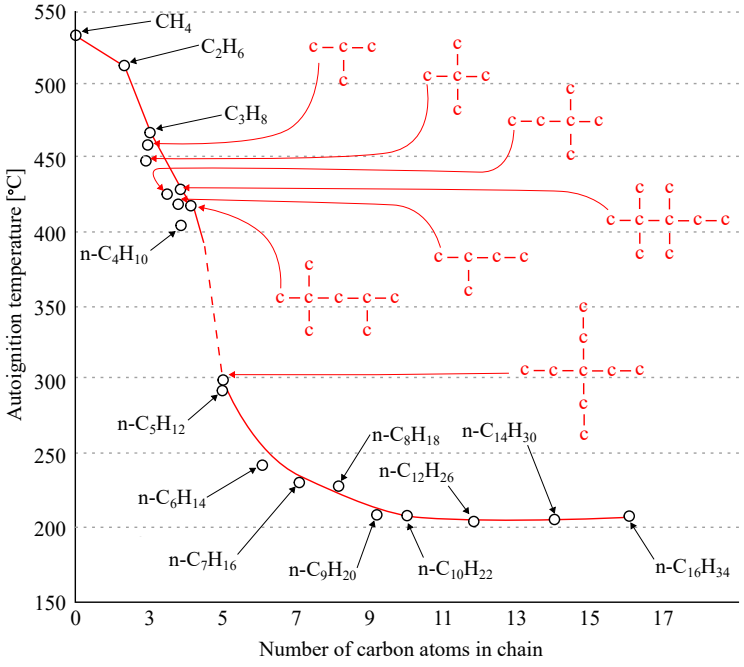

Figure 2.5. Autoignition temperature as a function of molecule carbon atoms [Fire Protection Association, 2014].

Methane, CH_4, has the highest AIT. Natural gas has a slightly lower AIT in atmospheric pressure, due to being a mix of mainly methane, ethane (C_2H_6) and propane (C_3H_8). It is relevant to be aware of this dependence on fuel in order to avoid unnecessary risk of ignition.

2.1.5 Turbulence

For non-premixed gas mixtures increased turbulence will help mix fuel and oxidiser. In the non-premixed case, turbulence increases the probability of ignition, which is utilised in commercial boilers to improve combustion. In premixed combustion turbulence ensure mixing of the hot products with the cold pre-mixed reactants, ensuring a continual combustion, a technique used in e.g. gas turbine combustion chambers [Boyce, 2011].

Very little information is available on the effect of turbulence on autoignition and even less on hot surface ignition [Markides, 2016]. Flow in gas turbines is generally characterised by a high turbulence intensity. Vlahostergiosa et al. [2015] concluded experimentally that increased turbulence intensity enhances heat transfer. The momentum exchange between the different parts of the turbulent boundary layer, causing the increased heat transfer, helps transferring heat and thereby mixing it better. It is likely that turbulence decreases the risk of ignition as the temperature of the fluid near the surface is cooler due to the mixing with the cold mean flow. Mullen II et al. [1948] measured HSITs of pentane/air flow over a hot rod and found that when they changed the upstream settings of the experimental set-up the HSIT was affected. It was not measured directly but Mullen II et al. [1948] suggested that upstream setting, theoretically leading to increased turbulence, corresponded with a measurable HSIT increase.

It is estimated that increased turbulence will increase the HSIT, but to what degree is still unknown, due to the lack of found papers analysing turbulence effect on hot surface ignition directly.

Cashdollar et al. [2000] investigated how turbulence effected the flammability limits and found a visible effect for hydrogen and no visible effect for methane. The LFL and UFL for hydrogen in atmospheric pressure and 25°C is shown in Table 2.2, for upward, downward and horizontal propagation direction, without the effect of turbulence.

	Lower limit (vol%)	Upper limit (vol%)
Upward propagation	4.1	74
Downward propagation	9.0	74
Horizontal propagation	6.0	74

Table 2.2. Flammability limits of hydrogen for different flame propagation directions [IAEA, 2011].

Turbulence in the gas flow will, according to IAEA [2011], widens the flammability domain. The effect of turbulence is to lower the LFL for downward and horizontal flame propagation

towards that of upward propagation. The overall effect on the flammability limits are therefore not critical when using flammability limits for safety margins to avoid ignition.

2.1.6 Residence time

The residence time is an expression of the time the gas mixture is in contact with the hot surface, being the surface contact length divided with the velocity. The lower residence time, the higher surface temperature is needed for ignition.

The effect of flow velocity on the HSIT is illustrated in Figure 2.6. In addition the effect of increased initial temperature is illustrated very well.

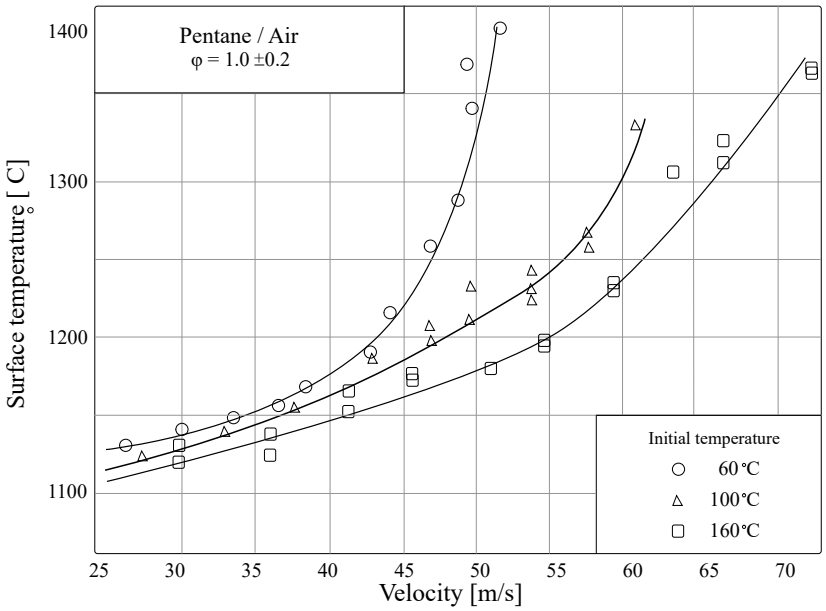

Figure 2.6. Hot surface ignition temperature (HSIT) of stoichiometric pentane/air mixture as a function of velocity and initial temperature [Mullen II et al., 1948].

The data presented in Figure 2.6 are determined by Mullen II et al. [1948] by experimental measurements on flow over a heated rod with a diameter of 1/4" (6.35 mm). The high velocities and small surface area cause the need for high HSITs.

2.2 State of the art hot surface ignition modelling

To determine how to model hot surface ignition a literature review is conducted.

A study by Üngüt [2001] with the title *CFD simulation and detailed chemical modelling of alkane autoignition near a heated metal surface* was contracted by HSE in order to address the risk of hot surface ignition in the industry. The fundamental procedure for determine the ignition risk was to separate simulating the fluid flow and the detail chemistry. A CFD flow simulation of the buoyant flow near a hot surface was performed and time history of local gas temperatures was calculated for 32 streamlines.

The temperature streamlines were provided as an input to the chemical kinetics program KISMET (KIneticS Modelling EnvironmenT) developed by Shell. Further details on KISMET and performance compared to CHEMKIN and experimental data are presented in the paper by Üngüt [2001]. KISMET integrates the chemical reactions along the streamlines. Figure 2.7 show the original streamline temperature profile together with the result of the KISMET calculation for a butane/air mixture and surface temperature of 1040 K.

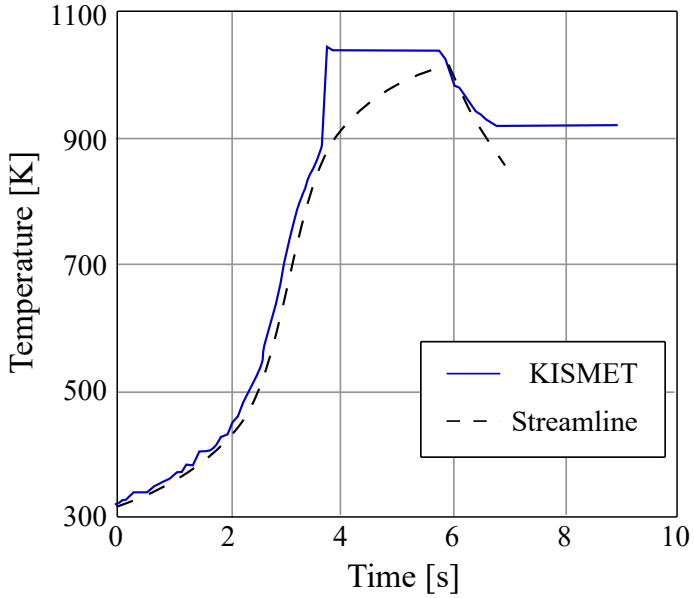

Figure 2.7. Time history of CFD streamline and KISMET calculated time history of buthane/air mixture and wall temperature of 1040 K [Üngüt, 2001].

The steep temperature gradient after approximately 3.5 seconds indicates that hot surface ignition has occurred. Üngüt [2001] determined HSIT of methane, propane, butane and natural gas in air for a stoichiometric range of 0.4 to 1.8.

In order to quantify the risk of ignition of gas flowing past a hot surface, Rasmussen and Sødring [2008] introduced the idea of the ignition parameter. When the ignition parameter, I_{gn}, is less then 1, no ignition is possible and when I_{gn} is greater than 1, ignition will occur. The ignition parameter is solved from Equation 2.2, on the standard transport equation form.

$$\frac{\partial\left(\rho I_{gn}\right)}{\partial t}+\frac{\partial}{\partial x_i}\left(\rho I_{gn} u_i\right)=\frac{\partial}{\partial x_i}\left(\Gamma_I \frac{\partial I_{gn}}{\partial x_i}\right)+S_{ign} \tag{2.2}$$

Where the ignition source term, S_{ign}, is given by Equation (2.3).

$$S_{ign}=\rho A \exp\left(\frac{-T_{act}}{T}\right)[fuel]^C\,[Air]^D-BI_{gn} \tag{2.3}$$

where:			
	A	Pre-exponential factor	$[s^{-1}]$
	T_{act}	Activation temperature	[K]
	C, D	Stoichiometric coefficient for fuel and air	[–]
	B	Sink term constant	$[kg/m^3\ s]$

The constants A, B, C, D and T_{act} are determined based on Equation (2.4) and relations between ignition delay, τ_{ign}, temperature and fuel/air mixture fraction, calculated by CHEMKIN. In Figure 2.8 this is illustrated for a mixture of natural gas and air.

$$\frac{1}{\tau_{ign}} = A \exp\left(\frac{-T_{act}}{T}\right) [fuel]^C [Air]^D - B\frac{RT}{MP} \tag{2.4}$$

where:			
	R	Ideal gas constant	[J/mol K]
	M	Molar mass of the gas mixture	[g/mol]
	P	Pressure	[Pa]

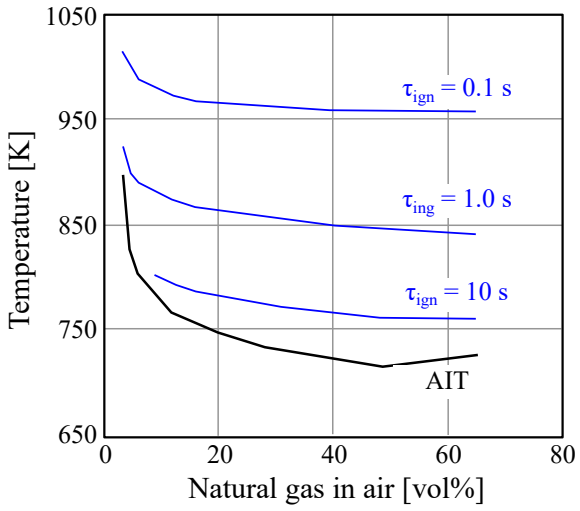

Figure 2.8. CHEMKIN calculated relations between ignition delay, temperature and fuel/air mixture fraction [Rasmussen and Sødring, 2008].

For more details on deriving the above mentioned equations, please refer to Rasmussen and Sødring [2008]. Conclusively the idea of the ignition parameter can be illustrated as in Figure 2.9 as a function of temperature and ignition delay time.

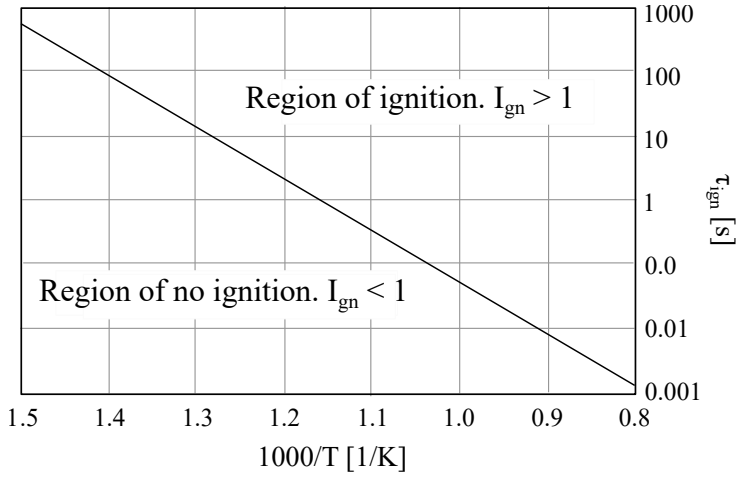

Figure 2.9. Illustration of the ignition parameter as a function of temperature and logarithmic ignition delay time, τ_{ign} [Rasmussen and Sødring, 2008].

Both Üngüt [2001] and Rasmussen and Sødring [2008] concluded a satisfactory coherence between modelled and measured HSITs. Common for both Üngüt [2001] and Rasmussen and Sødring [2008] is that the ignition delay time is used for determining hot surface ignition occurrence and that combustion is not included in their models. It is generally found that only few publications have been made regarding information and procedures to specifically model hot surface ignition and combustion.

Inspiration in order to develop a new model is found by extending the literature study to industries where understanding ignition and combustion is relevant. The following areas of interest were further reviewed:

- Explosion modelling at offshore oil and gas facilities
- Hydrogen ignition in nuclear facilities
- Pre-ignition modelling in engines

2.2.1 Explosion modelling at offshore oil and gas facilities

Several in-house and commercial models are available with a wide range of purpose and complexity [Lea and Ledin, 2002] [IAEA, 2011]. Model classes range from empirical, phenomenological to CFD and advanced CFD models. With advanced CFD models is meant that all obstacles are resolved in a 3D grid [Lea and Ledin, 2002].

In terms of modelling explosions on offshore oil and gas platforms focus tend to be on having a complex geometric representation and determine structural damage from deflagration/detonation overpressure or similar macro-physical properties.

The most used gas explosion model is the FLame ACceleration Simulator (FLACS) developed by GexCon in Norway since 1980 [Chillé et al., 2008]. FLACS is an advanced CFD tool used to model ventilation, gas dispersion, vapour cloud explosions and blast in complex process areas on offshore platforms [Chillé et al., 2008].

FLACS has a separated gas dispersion model. Results from the model include the time development of total amount of gas, amount of gas with concentrations within the flammability limits and amount of gas with concentrations close to stoichiometric [Chillé et al., 2008]. The amount of gas-air mixture that has concentration near stoichiometric is an interesting factor in safety analysis as it is related to overpressure [Vinnem, 2014]. Ignition is manually initiated in the code based on the gas dispersion model and a "worst case scenario" procedure. At time 0 half of the flammable mixture in a cell has undergone combustion causing a temperature increase starting ignition [Lees, 2012].

In the latest version of FLACS, it is possible to chose from two flamelets and a Burning Velocity Model (BVM) for either laminar, quasi-laminar or turbulent flow [Chillé et al., 2008]. The idea of using flamelets and the BVM to include detailed chemistry in a computationally easy way is adopted in this study. The theory behind flamelets and the BVM is presented further in Section 3.1.1. GexCon has performed over 2000 experiments in order to validate their FLACS code, so the use of flamelets and the BVM is assumed to be relatively well argued for.

The use of flammability as an ignition criteria was likewise found when investigating how hydrogen ignition in nuclear facilities is handled.

2.2.2 Hydrogen ignition in nuclear facilities

During severe accident in nuclear power plants, hydrogen igniting may lead to containment failure and leakage of radioactive material [Bielert et al., 2001]. Mitigation of hydrogen is for this reason implemented. Modelling and understanding hydrogen ignition specifically in nuclear power plants is an old topic in the literature. Sherman and Bergen [1987] used a quantitative ranking method to determine which combinations of geometry and mixture composition that can propagate detonation. Today mainly computational tools are used, as the combustion risk is dependent on the local hydrogen distribution demanding detailed modelling [IAEA, 2011]. Figure 2.10 shows the methodology to analyse hydrogen accident by HyCodes registered with Institute for Nuclear Energy Technologies, Forschungszentrum Karlsruhe (FZK) in Germany.

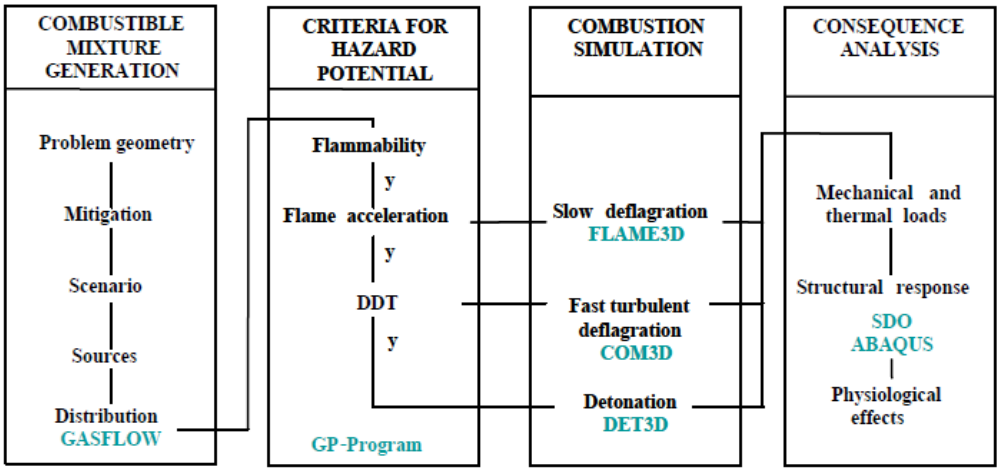

Figure 2.10. Methodology for analysing hydrogen behaviour during potential accidents scenarios by Sherman and Bergen [2005].

HyCodes, like GexCon, divide modelling into several sub-models. Gas distribution is handled by their code GASFLOW and dependent on the type of combustion, either the FLAME3D, COM3D or DET3D model is used. In addition a structural model handles the consequences in case of combustion.

Criteria for the hazard potential is handled by the GP-program. The GP-program contains information of flammability, flame acceleration and DDT (Deflagration-to-detonation) limits for different initial pressure, temperature and diluents concentration. All information is collected in a tabular form that is computationally light to handle [Bielert et al., 2001]. The GP-program by HyCodes inspired to develop a set of criteria for ignition. This far the flammability, utilised by HyCodes, and the ignition delay time, utilised by Üngüt [2001] and Rasmussen and Sødring [2008], seems like relevant criteria to include in that set.

2.2.3 Pre-ignition modelling in engines

The use of turbochargers and generally downsizing of Spark Ignition (SI) engines have increased the risk of uncontrolled ignition, referred to as pre-ignition [Zaccardi et al., 2009]. Zaccardi et al. [2009] investigated pre-ignition experimentally by measuring cylinder pressure over crank angle. Cycles with normal combustion and cycles with pre-ignition are easily separated. Pre-ignition has a higher pressure peak, oscillation pressure profile and occurs at a lower crank angle than normal combustion. Data on cycle pressure and crank angle gave basis for using robust statistics to analyse the risk of pre-ignition. In order to prevent pre-ignition in engines further analysis and understanding of the pre-ignition phenomena is needed [Zaccardi et al., 2009].

Different approaches have been taken in terms of modelling ignition. Fontanesi et al. [2013, 2014] used Large Eddy Simulation (LES) together with interpolative look-up approach for determining the ignition time delay. Linse et al. [2014] modelled the knocking phenomena in engines with the use of a model very similar to the BVM and flamelets method used in modelling explosions on offshore oil and gas facilities. Also in the model by Linse et al. [2014] the ignition time delay was stored in a table to ease computational time. By comparing with experimental data, Linse et al. [2014] concluded the model worked with "reasonable accuracy".

The cause of pre-ignition is due to the increase in temperature and pressure leading to either autoignition, hot surface ignition or ignition due to lubricating oil mixing with fuel [Kalghatgi and Bradley, 2012]. Kalghatgi and Bradley [2012] presented a different method in order to determine the risk of pre-ignition. In addition to a ignition time delay, a criterion for flame propagation was set up. For the risk of flame propagation, Kalghatgi and Bradley [2012] used the Zeldovich critical radius theory as a criterion for flame propagation. The theory was first presented by Zeldovich et al. [1985] and express that flame propagation is possible when the radius of the autoignited hot gas is greater than the critical radius for flame propagation which is proportional to the flame thickness. The flame propagation criterion is included in the model proposed in this study and described further in section 3.2.4.

An interesting conclusion from Kalghatgi and Bradley [2012] is that pre-ignition at a hot surface is caused by initiation of flame propagation and not autoignition.

The procedure of calculating the critical radius for flame propagation is based on calculating the critical radius of ignition, likewise presented in section 3.2.4. The critical radius of ignition is based on an assumption of the Van't Hoff to be valid.

Van't Hoff ignition criteria

The Van't Hoff criterion is well known in modelling particle combustion [Cassel and Liebman, 1963]. The criterion can be easily translated to be valid for ignition at a hot surface under the assumption that ignition occurs in the vicinity of the wall [Laurendeau, 1982]. An illustration of the Van't Hoff criterion is shown in Figure 2.11.

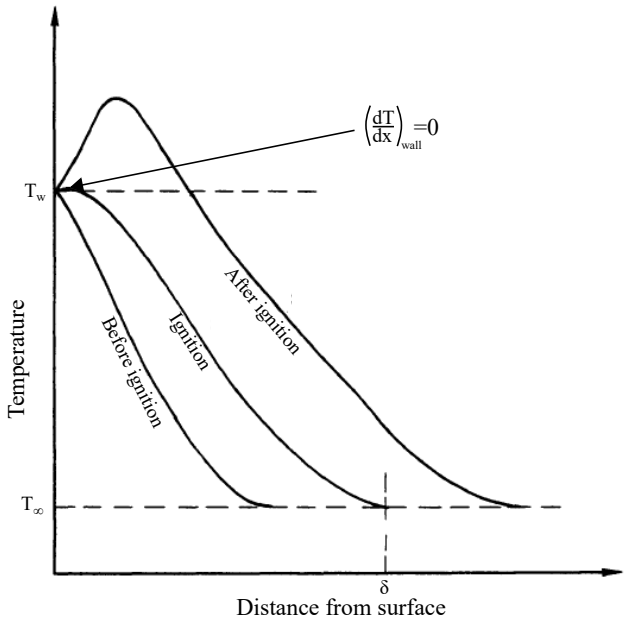

Figure 2.11. Illustration of the Van't Hoff criteria on hot surface ignition. Inspired by Laurendeau [1982].

The Van't Hoff criterion express that exactly at ignition the heat transfer from the wall equals the rate of heat generated by the chemical reactions resulting in a temperature gradient of 0 at the wall. This relationship can be used to calculate the minimum wall temperature that will ignite a passing flammable flow.

A derivation of the criterion and further explanation of the Van't Hoff are presented in 3.2.2.

2.3 Summary and project limitations

Hot surface ignition is a relatively complex mechanism that is affected by the physical and chemical conditions under which ignition is investigated. Most work focusses on determining the HSIT experimentally while changing preferably only one affecting parameter at a time.

The hot surface ignition models developed by Üngüt [2001] and Rasmussen and Sødring [2008] are both concluded to follow experimentally determined HSIT results relatively well for their specific ignition conditions tested. Similarly the flamelets and BVMs have been successfully implemented to model combustion on offshore oil and gas facilities and in engines [Chillé et al., 2008; Linse et al., 2014]. Mitigated hydrogen ignition in nuclear facilities is amongst others analysed in terms of flammability limits and fundamental understanding of Van't Hoff criterion of ignition opens for the possibility of determining a minimum wall temperature of ignition. Separately different academic and industrial researchers have shown successful modelling procedures that inspired to develop a model capable of analysing ignition and combustion characteristics of gas over a hot surface.

First steps toward developing a detailed CFD model capable of determining hot surface ignition and combustion are described in this study. Partly in order to get a working model within the time frame of a short master thesis and partly in order to develop a model that can be easily utilised by others, a simple model, requiring no extraordinary solver coding, is developed. The model is developed in ANSYS CFX, as it is the program used by LRC and UT, and has a well functioning toolbox for writing user defined functions (UDFs) in its CFX expression language (CEL).

3 CFD demonstration model

This chapter serves to present the demonstration model created in ANSYS CFX. The physical models used in CFX are presented in Section 3.1, with focus on the combustion models. Derivation and implementation of the ignition criteria and flame propagation criterion are presented in Section 3.2. In Section 3.3 the geometry and mesh are presented together with a mesh and time step sensitivity analysis. A short modelling summery are presented in Section 3.4 before simulation results are presented and discussed in Section 3.5. A discussion of the model applicability and sensitivity are presented in Section 3.6.

3.1 Physical models in CFX

Physical models of heat transfer, turbulence, radiation and combustion, listed in Table 3.1, are included in the demonstration model developed. Additional interesting simulation settings are listed in Appendix A.

Heat transfer model	Total Energy
Turbulence model	Shear Stress Transport (SST)
Radiation model	Discrete transfer
Combustion model	Burning Velocity Model (BVM)
	Laminar Flamelet with Probability Density Function (PDF)

Table 3.1. CFX physical models used in the demonstration model.

The Total Energy model is used for modelling the heat transfer. It has been chosen to include the effect of viscous heating and turbulence. The Total Energy transport equation model the enthalpy transport and is recommended by ANSYS, Inc [2016] for flow of gas.

The SST model is used to treat the turbulence in the demonstration model. It adds an extra equation to be solved but it includes the advantages of the k-ϵ model far from the wall and the advantages from the k-ω in the near wall region [Versteeg and Malalasekera, 2007]. Since the near wall modelling is very important for the demonstration model, this is prioritised.

A transport equation is solved for radiation in order to obtain a source term for the energy equation. Radiation modelling is time consuming due to its dependence on position, gradients and frequency [ANSYS, Inc, 2016]. Approximations is used to determine these dependencies. For cases involving optical thin regions, e.g. clear gas, to optical thick

region, e.g. combustion, ANSYS, Inc [2016] recommend to use either the Discrete Transfer or the Monto Carlo model. In the Discrete Transfer model multiple rays are tracked through the domain while in the Monto Carlo model its photons being tracked in the same way. The Discrete Transfer model is used with default settings for transfer mode and spectral and scattering model.

The combustion model included is the BVM modelling the progress of a global reaction and the Laminar Flamelet with PDF modelling the mixture composition. The theory behind the models and the coupling is presented in further details next.

3.1.1 Combustion model

Combustion modelling is a balance between including enough detailed chemistry and use a realistic computational time. A way to include a detailed chemistry while limit the computational time is to introduce the reaction progress variable, c. Instead of having a transport equation for all species involved, only one transport equation are added for c.

The reaction progress variable have a value between 0 and 1, where $c = 0$ correspond to fresh (unburnt) gas and $c = 1$ correspond to fully reacted (burned) gas. c is assumed to follow a bimodal distribution in turbulent flow. The gas mixture is at all times and positions assumed to be either fresh or fully burned. The average reaction progress variable, $\tilde{c}$, express the probability of the mixture being fully reacted. A $\tilde{c} = 0.6$ has to be understood so that the fluid is fully reacted 60% of the time and non-reacted the remaining 40% of the time at that position. This assumption is justified for fast chemistry combustion with Da$\gg$1 [ANSYS, Inc, 2016]. Notice the similarities to the ignition parameter, I_{gn}, used by Rasmussen and Sødring [2008] to model hot surface ignition. The averaged reaction progress variable, $\tilde{c}$, is computed by solving the transport equation (3.1).

$$\frac{\delta\left(\bar{\rho}\tilde{c}\right)}{\delta t} + \frac{\delta\left(\bar{\rho}\tilde{u}_j\tilde{c}\right)}{\delta x_j} = \frac{\delta}{\delta x_j}\left[\left(\overline{\rho D} + \frac{\mu_t}{\sigma_c}\right)\frac{\delta\tilde{c}}{\delta x_j}\right] + \bar{\omega}_c \tag{3.1}$$

where:			
	ρ	Density	[kg/m^3]
	c	Reaction progress variable	[–]
	t	Time	[s]
	u_j	Velocity component	[m/s]
	x_j	Directional component	[m]
	D	Mass diffusion	[m^2/s]
	μ_t	Turbulent dynamic viscosity	[Pa · s]
	σ_c	Turbulent Schmidt number with default value 0.9	[–]
	ω_c	Reaction source term	[kg/m^3 s]

Superscript meaning:

$\bar{}$	Reynolds averaged variable	[–]
$\sim$	Favre averaged variable	[–]

The more complex Favre averaging is used when the turbulent fluctuations lead to significant fluctuations in density. When using Favre averaging the variable is composed using a density weighted average [Cant and Mastorakos, 2008]. Equation (3.2) show the definition of Favre averaging the variable Φ.

$$\Phi = \widetilde{\Phi} + \Phi''$$

$$\tilde{\Phi} \equiv \frac{\overline{\rho\Phi}}{\overline{\rho}} \tag{3.2}$$

There are two models available in ANSYS CFX in order to define the reaction source term, $\overline{\omega_c}$, when modelling turbulent premixed or partial premixed combustion. The Burning Velocity Model (BVM), also known under the name Turbulent Flame Closure (TFC), and the Extended Coherent Flame Model (ECFM). The ECFM define the reaction source term in terms of the flame surface density. Calculating the flame surface density requires to solve another transport equation. The BVM is simpler, require no additional transport equations and used successfully on oil and gas facilities and in combustion engines to model combustion [Chillé et al., 2008; Linse et al., 2014]. The BVM is used in this demonstration model.

The reaction source term in the BVM is defined as Equation (3.3) and (3.4).

$$\overline{\omega_c} = \overline{S_c} - \frac{\delta}{\delta x_j}\left(\left(\overline{\rho D}\right)\frac{\delta \tilde{c}}{\delta x_j}\right) \tag{3.3}$$

$$\overline{S_c} = \overline{\rho_u} S_T |\Delta \tilde{c}| \tag{3.4}$$

where:	S_c	Combustion source term	[kg/m^3 s]
	ρ_u	Density of the unburnt mixture	[kg/m^3]
	S_T	Turbulent burning velocity	[m/s]

The mixture composition and the detailed reaction mechanism is handled by generating a flamelet library containing the mean species mass fractions, $\tilde{Y}_i$. The species mass fractions are related to the averaged reaction progress variable, $\tilde{c}$, by Equation (3.5)

$$\tilde{Y}_i = (1 - \tilde{c})\,\tilde{Y}_{i,fresh} + \tilde{c}\tilde{Y}_{i,burned} \tag{3.5}$$

where:	$Y_{i,fresh}$	Species mass fractions in the non-reacted fraction of the mixture	[–]
	$Y_{i,burned}$	Species mass fractions in the reacted/burned fraction of the mixture	[–]

The non-reacted species mass fractions, $Y_{i,fresh}$, are computed by a linear blending of the fuel and oxidizer input compositions. The burned species mass fractions, $Y_{i,burned}$, are computed by the flamelet model. In the flamelet model the turbulent flame is treated as an assemble of laminar thin sheets called flamelets. The advantages of the flamelet model

are that there is no need for a resolution that include the small length and time scales, resulting in a very robust method [ANSYS, Inc, 2016]. The flamelet model is restricted to be used on fast chemistry and under the assumption of a unity Lewis number.

The laminar chemistry is coupled with the turbulent flow field with the use of a statistical probability density function (PDF). The PDF is commonly agreed to have the shape of the Beta-PDF but any shape could be assigned if relevant [ANSYS, Inc, 2016]. The PDF is generated as a part of the process of generating the flamelet library and is not calculated during the CFD calculation.

The flamelet library give a tabulated Favre averaged mass fraction, $\tilde{Y}_i$, as a function of mean mixture fraction, $\tilde{Z}$, mixture fraction variance, $\tilde{Z"}^2$ and the scalar dissipation rate, $\tilde{X}$, as of Equation (3.6).

$$\widetilde{Y}_i = \widetilde{Y}_i\left(\widetilde{Z}, \widetilde{Z''}^2, \widetilde{X}\right) = \int_0^1 Y_i\left(\widetilde{Z}, \widetilde{X}\right) \cdot P_{\widetilde{Z},\widetilde{Z''}^2}(Z)\,\delta Z \tag{3.6}$$

where:	P	The PDF that couples the laminar chemistry to the turbulent flow field

Determining the mixture fraction mean and variance in the turbulent flow field is done be the transport Equations (3.7) and (3.8), respectively [ANSYS, Inc, 2016].

$$\frac{\delta\left(\bar{\rho}\widetilde{Z}\right)}{\delta t} + \frac{\delta\left(\bar{\rho}\widetilde{u_j}\tilde{Z}\right)}{\delta x_j} = \frac{\delta}{\delta x_j}\left[\left(\overline{\mu} + \frac{\mu_t}{\sigma_Z}\right)\frac{\delta\widetilde{Z}}{\delta x_j}\right] \tag{3.7}$$

$$\frac{\delta\left(\bar{\rho}\widetilde{Z''}^2\right)}{\delta t} + \frac{\delta\left(\bar{\rho}\widetilde{u_j}\widetilde{Z''}^2\right)}{\delta x_j} = \frac{\delta}{\delta x_j}\left[\left(\overline{\mu} + \frac{\mu_t}{\sigma_{Z''^2}}\right)\frac{\delta\widetilde{Z''}^2}{\delta x_j}\right] + 2\frac{\mu_t}{\sigma_Z}\left(\frac{\delta\widetilde{Z}}{\delta x_j}\right)^2 - \bar{\rho}\widetilde{X} \tag{3.8}$$

where:	μ	Dynamic viscosity	[Pa · s]
	σ_Z	Schmidt number with default value 0.9	[–]
	$\sigma_{Z"^2}$	Schmidt number with default value 0.9	[–]

The scalar dissipation rate is determined by the empirical expression in Equation (3.9).

$$\widetilde{X} = C_x\frac{\widetilde{\varepsilon}}{\widetilde{k}}Z''^2 \tag{3.9}$$

where:	C_x	Constant with default value 2.0	[s^{-1}]
	ε	Turbulent dissipation rate	[m^2/s^3]
	k	Turbulent kinetic energy	[m^2/s^2]

All reaction is suppressed until conditions for ignition and flame propagation is present in the fluid domain. Conditions for ignition and flame propagation is described next.

3.2 Ignition and flame propagation modelling approach

Ignition initiation is included in the model by setting up a set of criteria. Ignition will be initiated if:

- The mixture composition is within its flammability limits for the given temperature and pressure
- The surface temperature is above the minimum ignition temperature
- The ignition time delay is sufficiently small for ignition to occur over the surface size

The criteria are further described and derived in the sections 3.2.1 - 3.2.3. A criterion is similar set up for the risk of flames will propagate. If the criterion for flame propagation is fulfilled the combustion models are activated. The criterion for flame propagation is described in section 3.2.4.

3.2.1 Determination of flammability limits

Ignition is only possible when the mixture composition is within the flammability limits. At atmospheric pressure and 25°C the Lower Flammability Limit (LFL) and Upper Flammability Limit (UFL) for methane are 5.0 vol% and 15 vol%, corresponding to an equivalence ratio of 0.53 and 1.6, respectively [Coward and Jones, 1952]. The flammability limits are affected by temperature and pressure and in order to avoid unnecessary risk, calculation of flammability limits for specific ranges of temperature and pressure is needed. Note that the flammability limits are also important in the combustion model, as the flame speed is calculated based on the flammability limits in the BVM. Based on experimental data empirical correlation exists for temperature and pressure dependence on flammability limits.

The flammability limits vary nearly linearly with temperature [Zabetakis, 1999]. In accordance to the White criteria, saying that the flame temperature is constant at the lower limit, it is a fairly close assumption that the lower limit is a straight line, from the lower limit value at 25°C to the flame temperature [Zabetakis, 1999]. In this demonstration model the LFL is determined by the modified Burgess-Wheeler law, in Equation (3.10). The expression is valid for paraffin hydrocarbons, also known as alkanes, which are the main constituents in natural gas [Zabetakis, 1999].

$$L_T = L_{25^\circ} - \frac{0.75}{\Delta H_c}(T - 25^\circ) \tag{3.10}$$

where:	L_T	LFL at temperature T	[vol%]
	L_{25°	LFL at 25°C	[vol%]
	ΔH_c	Heat of combustion	[Kcal/mol]
	T	Temperature	[°C]

Heat of combustion and LFL at 25°C for methane, ethane and propane is shown in Table 3.2. The flammability limits are included in ANSYS CFX in terms of the equivalence ratio, λ, so the LFL value at 25°C is likewise presented in Table 3.2.

	ΔH_c [Kcal/mol]	L_{25° [vol%]	λ_{25° [–]
Methane	191.8	5.0	0.53
Ethane	341.3	3.0	0.53
Propane	488.5	2.1	0.52

Table 3.2. Properties of methane, ethane and propane [Zabetakis, 1999]. λ is the equivalence ratio.

Based on experimental measurement determining flammability limits of methane/air mixtures Vanderstraeten et al. [1997] developed a second order fit to calculate the pressure effect on the upper flammability limit. The expression is given in Equation (3.11).

$$UFL(p_1) = UFL(p_0)\left[1 + a\left(\frac{p_1}{p_0} - 1\right) + b\left(\frac{p_1}{p_0} - 1\right)^2\right] \tag{3.11}$$

where:			
	p_1	New pressure	[Pa]
	p_0	Original pressure	[Pa]

And where a and b are temperature dependent coefficients with values given in Table 3.3.

T [°C]	a [–]	a [–]
20	0.0466	-0.000269
100	0.0552	-0.000357
200	0.0682	-0.000541

Table 3.3. Temperature dependent coefficients a and b in Equation (3.11).

Implementation

Trends have been used to get a functions for the temperature coefficients a and b at the missing temperatures. The equations for the LFL and UFL are included via the CFX expression language (CEL). The LFL and UFL are included under *Reaction* → *Laminar Burning Velocity* in order to include the effect of temperature and pressure on the calculated laminar burning velocity. An if statement are set up in CEL so that the ignition delay time is only calculated if the mixture is in the flammable range and the wall temperature is high enough to cause ignition.

3.2.2 Determination of ignition temperature

The minimum wall temperature required for ignition can be derived based on the Van't Hoff criterion. The Van't Hoff criterion describe the temperature gradient from a wall before, under and after ignition. The illustration of the Van't Hoff criterion is shown in Figure 3.1.

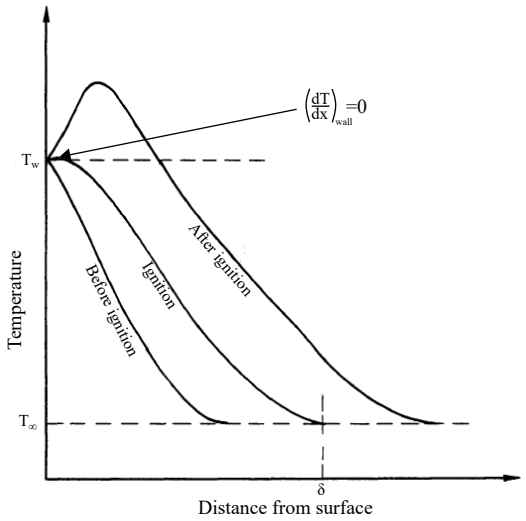

Figure 3.1. Illustration of the Van't Hoff criteria on hot surface ignition. Inspired by Laurendeau [1982].

Before ignition, heat transfer is from the wall to the flammable gas, while after ignition heat transfer is opposite, from the gas to the wall. The Van't Hoff criterion on ignition is that the temperature gradient at the wall equals 0. In other words ignition starts when the rate of heat loss to the surroundings equals that rate of heat generated by the chemical reaction, expressed as in Equation (3.12) [Laurendeau, 1982].

$$q_{loss} = q_{chem} \tag{3.12}$$

where:			
	q_{loss}	Rate of heat losses to the surroundings	[J/m^2 s]
	q_{chem}	Rate of heat generated by the chemical reaction	[J/m^2 s]

In addition to the Van't Hoff criterion to be valid the following major assumptions for the use of this method are [Laurendeau, 1982]:

- Chemical reactions occur in the vicinity of the hot surface
- Chemical kinetics can be described by an single overall chemical reaction
- No reactant depletion occurs until ignition
- Physical properties are evaluated at a geometric mean temperature

The heat loss to the surroundings, q_{loss}, can be determined by the engineering correlation in Equation (3.13).

$$q_{loss} = \frac{kNu}{L}(T_w - T_\infty) \tag{3.13}$$

where:			
	k	Thermal conductivity	[J/m K]
	Nu	Nusselt number	[–]
	L	Characteristic length of the hot surface	[m]
	T_w	Wall temperature	[K]
	T_∞	Ambient temperature	[K]

The Nusselt number expresses the ratio of convective to conductive heat transfer across the boundary layer. Empirical expressions for Nusselt number, Nu, are available for several geometries and for stagnant, free and forced convection. In this demonstration model the Gnielinski correlation, in Equation (3.14), for turbulent pipe flow is adopted.

$$Nu_D = \frac{(f/8)(Re_D - 1000)Pr}{1 + 12.7(f/8)^{1/2}\left(Pr^{2/3} - 1\right)} \tag{3.14}$$

where:	f	Friction factor	[–]
	Pr	Prandtl number	[–]
	Re	Reynolds number	[–]
Subscript meaning:			
	D	Referenced to the hydraulic diameter	[m]

The friction factor, f, can be found from Moody chart or Petukhov's correlation for smooth tubes in Equation (3.15).

$$f = (0.79\ln(Re_D) - 1.64)^{-2} \tag{3.15}$$

The equation for heat losses to the surroundings do not include radiation. At high temperatures it might be relevant to include. A relative simple way could be to introduce a total Nusselt number, which is the sum of a radiative and a convective Nusselt number, in the heat loss Equation (3.13). A correlation for a radiative Nusselt number, as a function of optical thickness and Reynolds number, is amongst others suggested by Galarça and França [2007].

The Prandtl number, Pr, is the ratio of momentum and thermal diffusivity and given as Equation (3.16).

$$Pr = \frac{\nu}{\alpha} = \frac{c_p \mu}{k} \tag{3.16}$$

where:	ν	Kinematic viscosity	[m^2/s]
	α	Thermal diffusivity	[m^2/s]
	c_p	Specific heat at constant pressure	[J/kg K]
	μ	Dynamic viscosity	[kg/m s]
	k	Thermal conductivity	[W/m K]

The pipe Reynolds number, Re_D, is calculated by Equation (3.17).

$$Re_D = \frac{\mathrm{v} D_H}{\nu} \tag{3.17}$$

where:	v	Mean velocity	[m/s]
	D_H	Hydraulic diameter	[m]

The heat rate due to chemical reactions is derived from the energy equation at the surface at ignition, as of Equation (3.18).

$$k\frac{d^2T}{dx^2} + Qr_f = 0 \tag{3.18}$$

where:			
	T	Temperature	[K]
	x	Distance from surface	[m]
	Q	Heat of combustion	[J/mol]
	r_f	Molar reaction rate	[mol/m^3 s]

Where the molar reaction rate is given by Equation (3.19).

$$r_f = -X_F^{m_f} X_O^{m_o} \rho^n A exp(-E_a/RT) \tag{3.19}$$

where:			
	X_F	Mole fraction of fuel	[mol/mol]
	X_O	Mole fraction of oxidiser	[mol/mol]
	m_f	Partial order with respect to fuel	[–]
	m_o	Partial order with respect to oxidiser	[–]
	ρ	Density	[mol/m^3]
	n	Overall reaction order, $n = m_f + m_o$	[–]
	A	Frequency factor	[[mol/m^3]$^{1-\mathrm{n}}$s^{-1}]
	E_a	Activation energy	[J/mol]
	R	Universal gas constant	[J/mol K]

The heat rate from chemical reactions is derived by integrating the above expressions over the thermal boundary layer with the following boundary conditions:

$$x = 0, \qquad T = T_w$$
$$x = \delta, \qquad T = T_\infty$$

The final result is given by Equation (3.20). For details on deriving the expression, please refer to Laurendeau [1982] or Boettcher [2012].

$$q_{chem} = \sqrt{2kAQX_F^{m_f} X_O^{m_o} \rho_\infty^n \left(\frac{T_\infty}{T_w}\right)^{n/2} \exp\left[-\frac{E_a}{RT_w}\right] \left(\frac{RT_w^2}{E_a}\right)} \tag{3.20}$$

where:			
	ρ_∞	Ambient density	[mol/m^3]

Implementation

The criterion is included in the if statement calculating the ignition time delay. The ignition time delay is calculated if the mixture is within the flammability limits and if $q_{chem} \geq q_{loss}$. If the criterion is not fulfilled the ignition time delay is set artificially high, so no ignition occurs.

3.2.3 Determination of the ignition time delay

Ignition delay time can be determined experimental or from knowledge of the complex kinetics. In this demonstration model a correlation for methane-air as a function of temperature, pressure and equivalence ratio is used. The correlation, in Equation 3.21, is developed by Hu et al. [2015] based on fitting to experimental data.

$$\tau_{ign} = 1.09 \cdot 10^{-3} P^{-0.68} \phi^{0.04} \exp\left(\frac{40.98 \pm 0.51[\text{kcal} \cdot \text{mol}^{-1}]}{RT}\right) \tag{3.21}$$

where:			
	τ_{ign}	Ignition time delay	[μs]
	P	Pressure	[atm]
	ϕ	Equivalents ratio	[–]
	R	Universal gas constant = $1.986 \cdot 10^{-3}$	[kcal/(mol K)]
	T	Temperature	[K]

The experimental range of Hu et al. [2015], for which the correlation is applicable, is a temperature range of 1300-1900 K, a pressure range of 1-10 atm and a equivalence ratio range of 0.5-2.0.

Implementation

Autoignition models are available in ANSYS CFX. With the use of BVM the autoignition knock model is possible to enable. The source term, $S_{c,knock}$ given by Equation (3.22), is added to the reaction progress transport equation [ANSYS, Inc, 2016].

$$S_{c,knock} = \overline{\rho}\,(1 - \tilde{c})\, A_{knock} \exp\left(-E_{A,knock}/\left(RT\right)\right) \delta\left(\tilde{R} - 1\right) \tag{3.22}$$

where:			
	A_{knock}	Pre exponential factor	[s^{-1}]
	$E_{A,knock}$	Activation energy	[J/mol]
	$\tilde{R}$	Elapsed fraction of ignition delay time	[–]
	$\delta\left(\tilde{R} - 1\right)$	Step function that equals 0 if $\tilde{R}<1$ and equals 1 if $\tilde{R}>1$	[–]

The elapsed fraction of ignition delay time, $\tilde{R}$, is solved by the transport equation (3.23), which account for the varying ignition time delay, τ_{ign}.

$$\frac{\delta\left(\bar{\rho}\tilde{R}\right)}{\delta t} + \frac{\delta\left(\bar{\rho}\tilde{u}_j\tilde{R}\right)}{\delta x_j} = \frac{\delta}{\delta x_j}\left[\left(\overline{\rho D} + \frac{\mu_t}{\sigma_c}\right)\frac{\delta\tilde{R}}{\delta x_j}\right] + \frac{\bar{\rho}}{\tau_{ign}} \tag{3.23}$$

The implementation ensure that no ignition is initiated before the $\tilde{R} \geq 1$ translating to no ignition occurs before the ignition delay has expired.

As the last the flame propagation criterion is derived and implemented.

3.2.4 Flame propagation criterion

Ignition is defined as the transformation from non-reacted flammable material to a self-propagating state. By self-propagating state is understood that combustion continues when the source of ignition is removed.

The Zeldovich critical radius theory is adopted in order to model the risk of flame propagation from hot surface ignition. The theory was first presented by Zeldovich et al. [1985] and express that flame propagation is possible when a critical radius of burnt hot gas is proportional to the flame thickness. The Zeldovich theory is expressed in Equation (3.24).

$$\frac{r_f}{\delta_f} = \exp\left(\frac{\beta}{2}\left(1 - \frac{1}{\mathrm{Le}}\right)\right) \tag{3.24}$$

where:			
	r_f	Critical radius of hot pocket of burned gas	[m]
	δ_f	Laminar flame thickness	[m]
	β	Zeldovich number	[–]
	Le	Lewis number	[–]

Where the Zeldovich number is calculated by Equation (3.25).

$$\beta = \frac{E_a(T_b - T_u)}{R\,T_b^2} \tag{3.25}$$

where:			
	E_a	Activation energy	[J/mol]
	T	Temperature	[K]
	R	Universal gas constant	[J/mol K]

Subscript meaning:

b	Burnt mixture	[–]
u	Unburnt mixture	[–]

The Lewis number express the ratio of thermal and mass diffusivity, characterising the fluid flow where there are both heat and mass transfer. The Lewis is often assumed a value of unity in gas combustion modelling as it simplifies the calculation considerably. The assumption is amongst others used in the flamelet combustion model used in this demonstration model. With the assumption of unit Lewis number the Zeldovich theory can be simplified to Equation (3.26).

$$r_f = \delta_f \tag{3.26}$$

The flame thickness is determined as a correlation to save computational time. The approximation used is Blint's correlation, Equation (3.27), which include a correlation for the burned gas properties [Vancoillie et al., 2012].

$$\delta_f = 2\,\frac{\alpha}{S_L}\,\left(\frac{T_b}{T_u}\right)^{0.7} \tag{3.27}$$

where:	α	Thermal diffusivity	[m^2/s]
	S_L	Laminar flame speed	[m/s]

The critical radius for flame propagation, r_f, is calculated based on the critical Frank-Kamenetskii (F-K) parameter, δ_c. The critical F-K parameter depends on geometry and activation energy and can be used to determined the critical radius of ignition, r_c, as in Equation (3.28) [Bradley, 1996].

$$r_c = \left(\frac{\delta_c k T_\infty}{AQE_n \exp(-E_n)} \right)^{1/2} \tag{3.28}$$

where:	Q	Heat of combustion	[J/kg]
	E_n	Dimensionless activation energy $E_n = E_a/RT_\infty$	[–]

The value of the critical F-K parameter for a flat plate is shown in Figure 3.2 as a function of E_n.

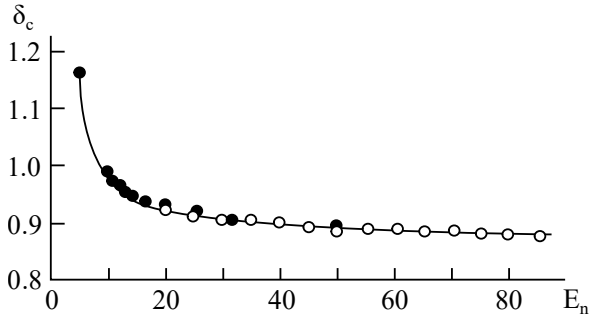

Figure 3.2. Value of the critical F-K parameter, δ_c, as a function of the dimensionless activation energy, E_n [Takeno, 1977].

Under assumption of the mixture behaving as an ideal gas, the critical volume can be calculated after ignition has occurred. The effect of change in pressure is neglected, so the critical volume of flame propagation can be calculated by Equation (3.29).

$$V_f = \frac{T_b}{T_u} V_c \qquad \Rightarrow \qquad r_f = r_c \left(\frac{T_b}{T_u} \right)^{1/2} \tag{3.29}$$

where:	V_f	Critical volume for flame propagation	[m^3]
	V_c	Critical volume for ignition	[m^3]
	T_b	Burnt gas temperature	[K]
	T_u	Unburnt gas temperature	[K]

The critical radius of flame propagation can then be compared with the laminar flame thickness.

Implementation

The criterion for flame propagation is included in the demonstration model by an expression for calculating the reaction rate. If the criterion is not fulfilled, and no reaction has occurred already, the reaction rate is set to be 0 $\mathrm{kg/m^3}$ s. If the criterion is fulfilled the reaction rate is calculated as by Equation (3.19) used in determine the heat rate from chemical reactions in Section 3.2.2. The calculated reaction rate is implemented by enabling the *Customise Knock Reaction Rate* in the autoignition model in CFX. In the knock source term equation, Equation (3.22), the part $A_{knock} \exp\left(-E_{A,knock}/\left(RT\right)\right)$ is replaced with the custom calculated reaction rate. From this step forward the combustion model takes over automatically.

3.3 Model geometry and mesh

The baseline case for modelling hot surface ignition is the experimental set-up at University of Twente (UT) in the Netherlands. It could be of interest to modify this existing set-up in case experimental validation of a numerical model becomes possible.

3.3.1 Experimental set-up at University of Twente

The experimental set-up at UT is originally designed to investigate flame propagation in combustion chamber and consists of a pre-heater, a combustion reactor and a gas cooler shown in Figure 3.3.

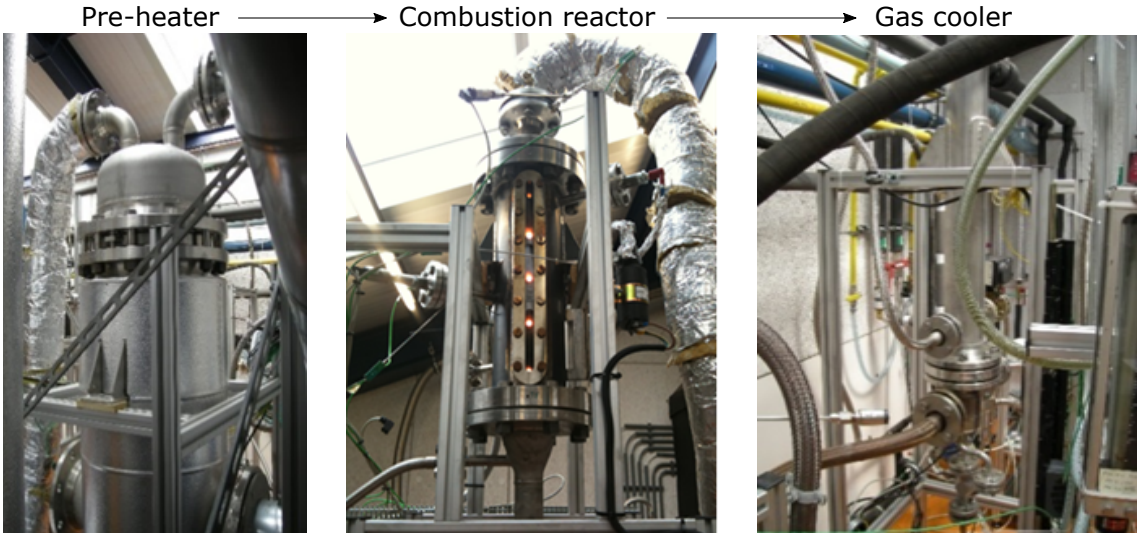

Figure 3.3. Experimental set-up at University of Twente.

Input to the pre-heater is public natural gas from the local gas distributor. Premixed compressed air and natural gas, with equivalence ratio between 0.5 and 1, are led into the pre-heater.

The pre-heater can heat the gas mixture up to 400°C and pressurise it up to 6 bar [Lloyd's Register Consulting, 2016a]. Gas is feed through a swirler before entering the combustion reactor.

The combustion reactor has a stainless steel case over a ceramic liner with an optical access through a quartz glass covered hole. A schematic of the combustion reactor is shown in Figure 3.4.

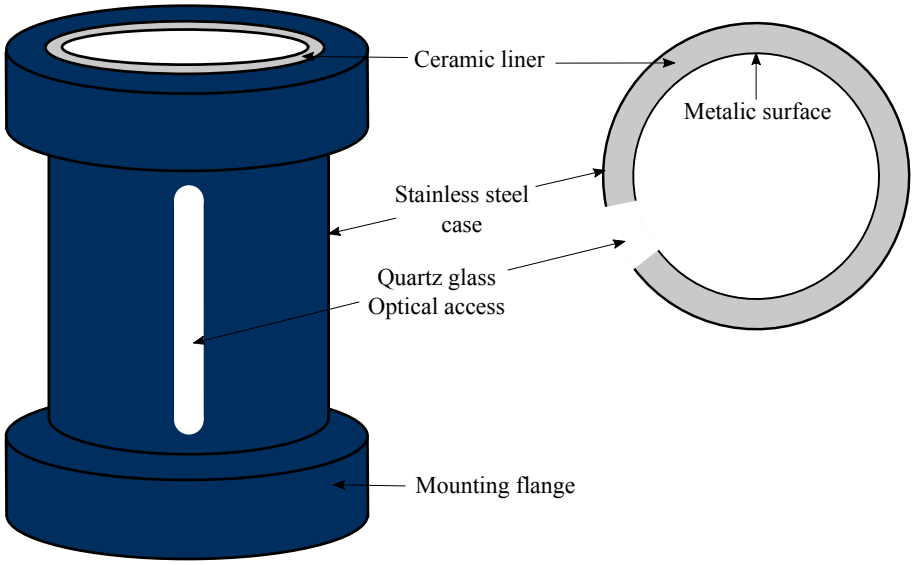

Figure 3.4. Schematic of the combustion reaction in the experimental set-up.

The cylindrical combustion reactor has a length of 500 mm and an outer diameter of 100 mm. In order to test hot surface ignition custom built ceramic liners with different inner diameter and different inner metal surface are to be constructed when designing the tests.

In order to investigate hot surface ignition in the existing set-up a burner ahead of the test section can initially burn natural gas to heat up the ceramic liner and metal surface. The temperature of the ceramic liner can be heated up to 1127°C (1400 K). The flame can be extinguished by cutting the natural gas supply. The natural gas can then be enabled again to simulate a gas leak passing a hot surface. The hot surface being the inner metallic surface in this set-up. The gas mixture can either be led through the swirler or be bypassed affecting the flow characteristics able to test.

The exhaust gas is led from the combustion reactor to the gas cooler for cooling before being led out.

3.3.2 Computational domain

The computational geometry, representing the experimental set-up at UT, consists of a simple cylinder flow domain. The optical access is not included in the model geometry making it a full cylinder surface. With the complete symmetry the fluid domain is simplified to a 20° section of the original as illustrated in Figure 3.5.

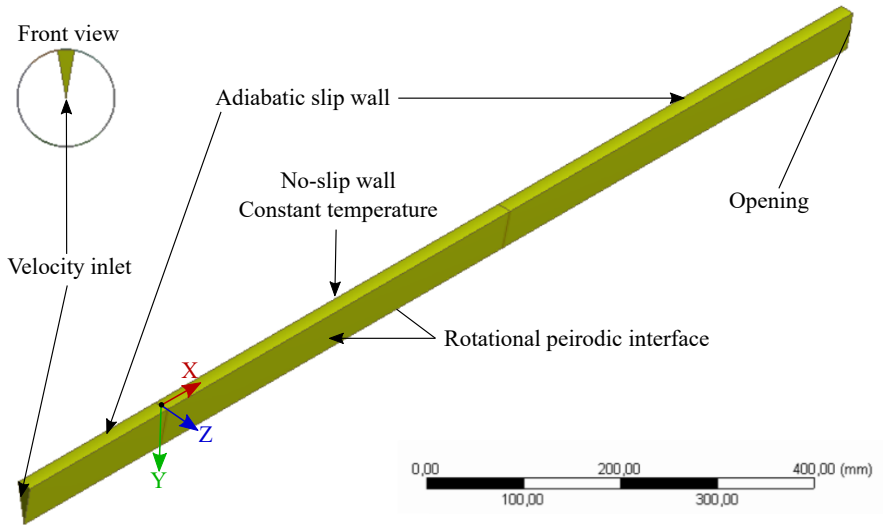

Figure 3.5. Computational domain.

The combustion reactor wall is a no slip wall and assigned a constant temperature. An entry and exit region is included at the inlet and outlet of the combustion reactor to limit potential effects hereof. The interfaces inside the fluid domain is assigned a rotational symmetry around the z axis. The rotational symmetric interface ensures physical flow characteristic while saving computational time. The outlet of the computational domain is assigned as an opening. The inlet is a velocity inlet. In order to include the effect of the swirler at the combustion reactor inlet, velocity is included in cylindrical coordinates with values of axial and tangential direction.

3.3.3 Mesh and time step sensitivity analysis

A mesh sensitivity analysis is conducted in order to understand mesh influence on the solution. An overview of the different meshes designed for the mesh sensitivity analysis is presented in Table 3.4. The number of nodes and elements are for the 20 degree computational domain.

	Mesh -3	Mesh -2	Mesh -1	Mesh 0	Mesh +1	Mesh +2
Nodes	321,994	446,949	551,588	1,017,875	1,926,683	3,873,600
Elements	66,600	96,000	119,825	226,164	438,949	898,800
y^+	36.94	15	9	4.56	1.42	0.68

Table 3.4. CFX physical models used in the demonstration model. The value of y^+ is area averaged over the no slip wall at the time step prior to ignition.

Due to high temperature gradients and combustion occurring at the wall a fine boundary layer resolution is needed. Ignition timing as a function of y^+ is presented in Figure 3.6. Ignition time are defined as the first time step where the reaction progress variable has a value higher than zero.

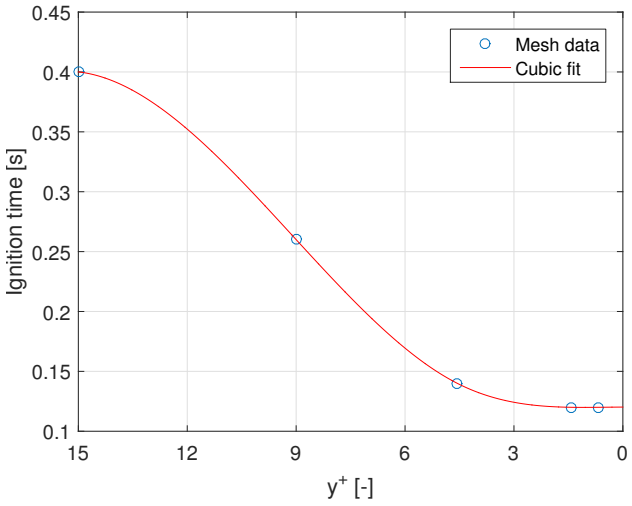

Figure 3.6. Ignition timing as a function of y^+.

No ignition is witnessed in the mesh -3 and it is therefore not included in Figure 3.6. It is seen that as y^+ is in the approximate range of 0-2 the ignition time reach a stable value of 0.11 s. In addition to the ignition time also the ignition position is changing with the mesh. As the mesh gets finer the position of ignition moves upstream. An illustration of this is presented in Figure 3.7, showing the reaction progress variable at different time steps and along the wall for the mesh -1 and +1. The position -0.2 m to 0 m correspond to the entry zone, 0 m to 0.5 m is the heated no slip wall and from 0.5 m to 1 m is the exit zone.

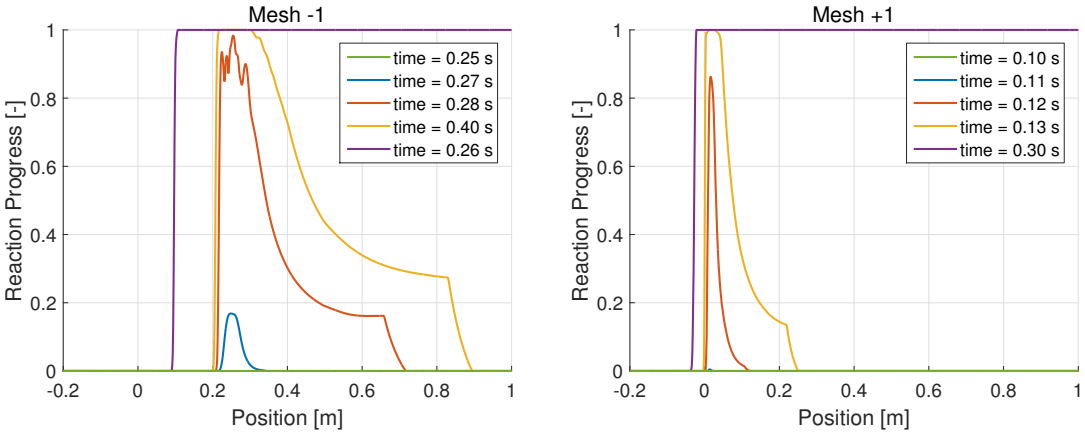

Figure 3.7. Reaction progress variable as a function of time and position for mesh -1 and mesh +1, respectively.

The position of ignition does not change between mesh +1 and mesh +2. The development of combustion is very mesh dependent and there is a visible difference between the two mesh, as can be seen in Figure 3.8.

If the purpose of the model is to investigate the risk of ignition, the mesh +1 is sufficient. If interest is on the combustion development right after ignition, finer meshes are needed to be analysed until no mesh influence is visible.

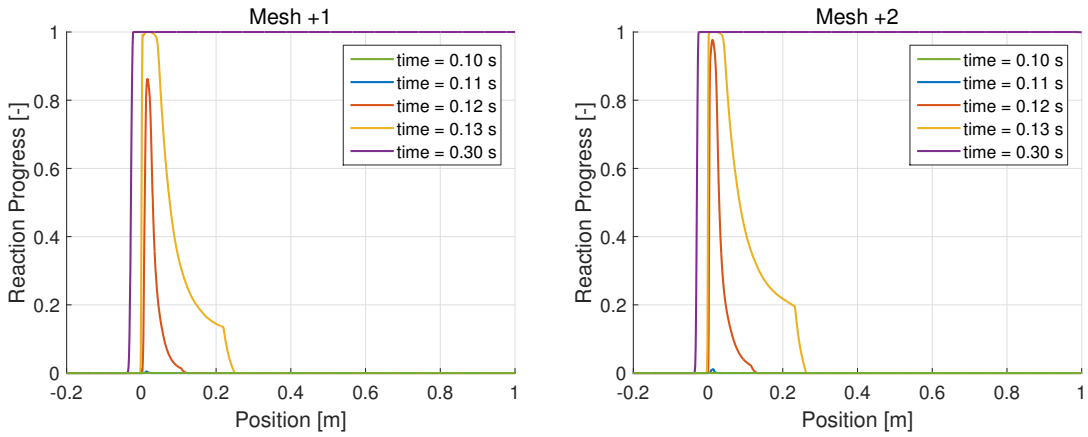

Figure 3.8. Reaction progress variable as a function of time and position for mesh +1 and mesh +2, respectively.

This demonstration model and thesis in general focus mainly on developing a model that potentially can be used to predict the risk of hot surface ignition, and it is decided to work on with the +1 mesh.

On the mesh a time step sensitivity analysis is conducted. An overview of the time step tested is collected in Table 3.5. Time step size of 10 ms correspond to the time step of the mesh sensitivity analysis.

Run	Time step Δt [ms]	Courant number* [-]	Ignition time [s]
1	10.0	106.4	0.11
2	1.0	11.1	0.107
3	0.5	3.8	0.103

Table 3.5. Time step sensitivity analysis runs. *The courant number given is the maximum value in the fluid domain.

The courant number is a measure of number of mesh elements the fluid passes over in one time step and a usable parameter in transient simulations. The courant number is determined by Equation (3.30).

$$C = \Delta t \sum_{i=1}^{n} \frac{u_{x_i}}{\Delta x_i} \tag{3.30}$$

where:			
	C	Courant number	[–]
	Δt	Time step size	[s]
	n	Dimensions	[–]
	u	Velocity	[m/s]
	Δx	Length interval	[m]

The time step must be small enough to resolve the time dependent features which depend on the problem being simulated. Typical values of the courant number are between 2-10,

but higher values can be accepted for some problems [ANSYS, Inc., 2009]. Combustion modelling often require a low courant number in order to capture the fast chemical kinetics.

The reaction progress variable as a function of position and time is presented in Figure 3.9 for simulations with time step size 10, 1 and 0.5 ms.

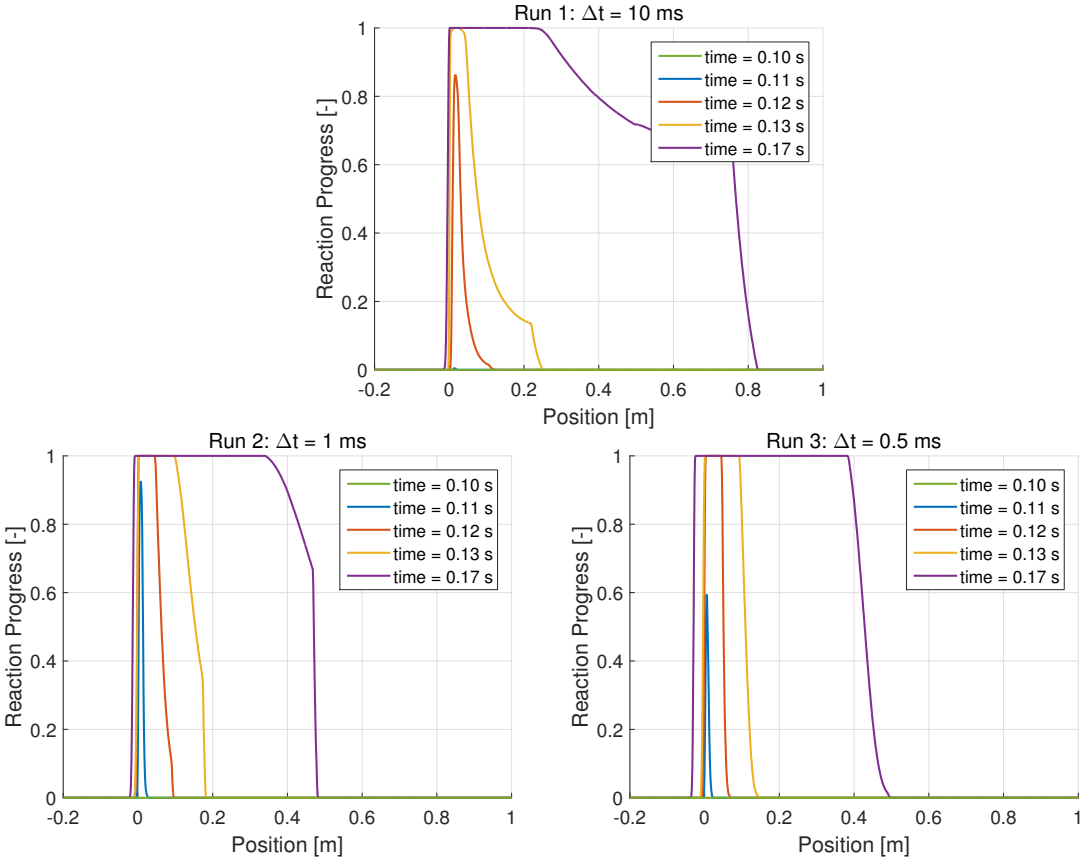

Figure 3.9. Reaction progress variable as a function of time and position with a time step size of 10 ms, 1 ms and 0.5 ms, respectively.

It can be seen from Figure 3.9 that the ignition is initiated in the step between 0.10 and 0.11 seconds for all runs. From Table 3.5 can it be read off that the ignition timing for run 3, with time step size of 0.5 ms, is 4 ms earlier than for run 2, with time step size of 1 ms. It is interesting that Figure 3.9 show combustion is further developed in run 2 rather than for run 3. It is observed that run 3 at time 0.17 s has developed a little more upstream relative to run 2. Generally it seems that the combustion time dependent features is not fully resolved, causing the combustion part to be over predicted.

With the simulation focus on the capability of predicting hot surface ignition a time step of 10 ms seems proficient. The maximum courant number is relatively high, but as no serious convergence problems have arrived during simulations and focus is in the near wall region having a lower velocity (and thereby lower courant number), it is tolerated as for now.

3.4 Modelling summery

The developed ignition initiation procedure is illustrated in the flowchart in Figure 3.10.

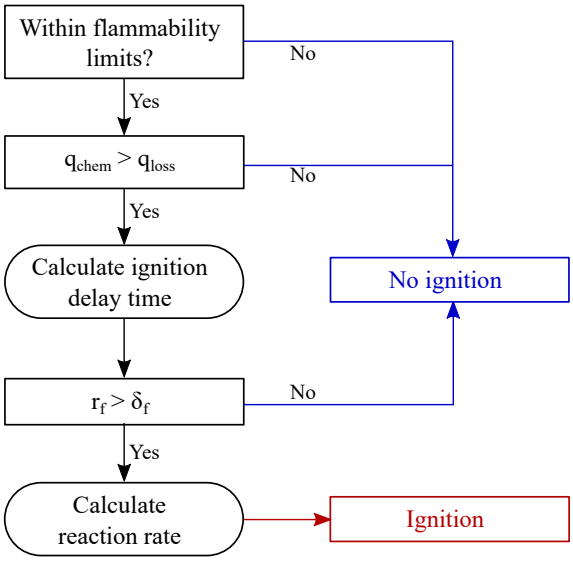

Figure 3.10. Flowchart describing the ignition initiation procedure.

If no ignition is initiated the combustion source term in the energy transport equation is zero. If ignition is initiated the reaction progress is determined by the BVM and the flamelet combustion models. Ignition initiation is defined by the time step and position where the reaction progress variable first has a value above zero.

It was clear from the mesh and time step sensitivity analyses that if modelling focus is on the combustion process a fine mesh and time step is required due to the large and fast changes. With focus on ignition initiation a more rough mesh and time step can be chosen to save computational time. When ignition initiation is known an additional simulation could be conducted with a refined mesh and time step in the range around ignition.

3.5 Simulation results

In order to investigate how the HSIT is affected by changes in the flow conditions, simulations are conducted with varying:

- Inlet velocity
- Turbulence intensity
- Initial temperature
- Pressure

It is interesting to investigate if the model delivers reasonable and physical results. These parameters are chosen as high values of each are characteristic for the flow in gas turbines. The simulation results are presented in the following with a discussion of interesting model responses. A collection of all simulations are presented in Appendix B.

3.5.1 Inlet velocity influence on the HSIT

HSIT results for simulating with variable inlet velocity are shown in Figure 3.11.

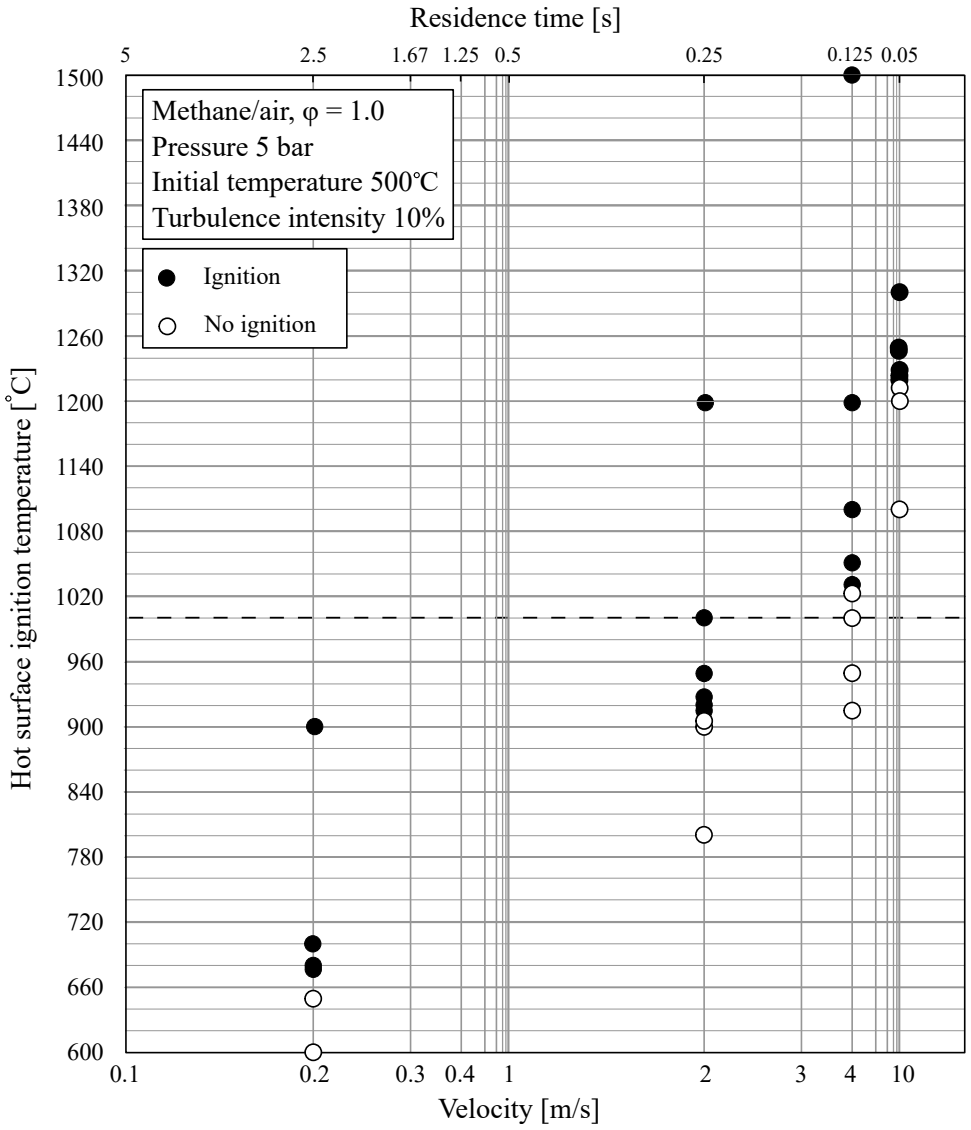

Figure 3.11. Simulation results illustrating the effect of changing inlet velocity on the HSIT.

As the inlet velocity increases and the residence time thereby decreases, the HSIT increases. This corresponds with expectations based on available literature. As the residence time decreases, a higher wall temperature is required to heat up the gas to the temperature where it will ignite. The lower residence time requires faster heat transfer which can be archived by increasing the temperature difference between gas and wall.

According to Boyce [2002] and Pedersen [2005] highest surface temperatures present in gas turbine are about 1000-1100°C. Surface temperatures of 1000°C, were confirmed by GE Oil & Gas [2016] in their gas turbines. HSIT of 1000°C is marked by a black dashed line in Figure 3.11. With inlet velocity above 4 m/s a hot surface temperature of 1000°C will not ignite the flammable mixture. The highest surface temperatures in the gas turbine are found in the combustion chamber and the first stage of the high pressure (HP) turbine [GE

Oil & Gas, 2016]. Preliminary modelling from Lloyd's Register Consulting [2016a] estimate velocities of 35 m/s between the combustor liner and casing under normal operation. At such high velocities the surface temperature of 1000°C will not ignite a flammable gas passing the hot surface. As the gas turbine is shut down the velocity decreases. Fast shutdown can be problematic if for example it decreases below 0.2 m/s faster than the combustor liner temperature drops below 675°C. Another risk is associated with local recirculation zones or stagnant flow zones that risk occurring near hot surfaces earlier in the shutdown procedure.

3.5.2 Turbulence intensity influence on the HSIT

The impact on the HSIT with change in the turbulence intensity is shown in Figure 3.12.

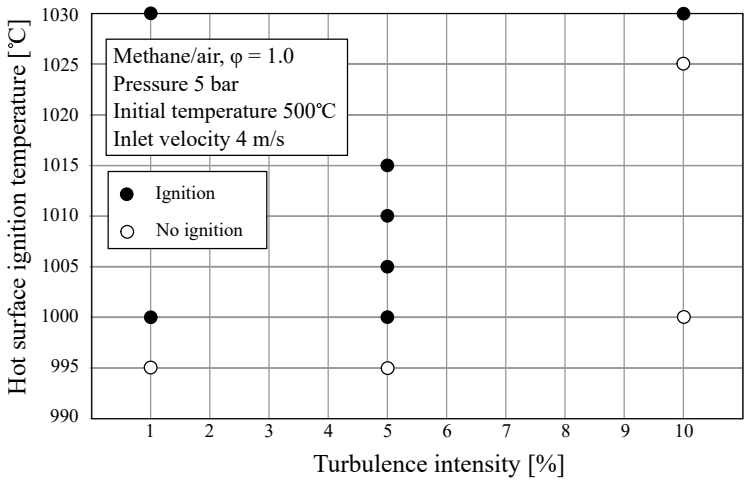

Figure 3.12. Simulation results illustrating the effect of changing turbulence intensity on the HSIT.

Turbulence is added to the simulation by giving a value for turbulence intensity in the initialisation and the velocity inlet. The turbulence intensity, I, is defined as in Equation (3.31).

$$I \equiv \frac{u'}{U} \tag{3.31}$$

where:	u'	RMS of the turbulent velocity fluctuations	[m/s]
	U	Mean velocity	[m/s]

A turbulence intensity of 1%, 5% and 10%, correspond to a low-, medium- and high-turbulence case, respectively.

Simulations are done until a difference of 5°C on ignition and no ignition is observed. For a turbulence intensity of 1% and 5% no change in the HSIT range is observed. This may be because the temperature resolution is too rough to determine any difference or simply because there is no difference in HSIT.

A difference of 10 ms is observed in ignition timing for a turbulence intensity of 1% and 5%, as shown in Table 3.6. This illustrates that the increased turbulence might affect in a degree not dissolved by the mesh, time step or temperature range simulated.

Initial temp.	HSIT [°C]	Ign. time [s]
1%	1000	0.26
5%	1000	0.27
10%	1030	0.25

Table 3.6. HSITs and ignition time as a function of initial temperature.

With a turbulence intensity of 10% the HSIT increases by 30°C compared to when the turbulence intensity is 1% or 5%. Increased turbulence intensity leads to increased turbulent eddies cooling the gas in the near wall region. It seems this tendency leads to increased HSITs. The estimated tendency of HSIT with increased turbulence observed by Mullen II et al. [1948] is similarly observed in the simulation results.

The turbulence intensity is typically high in gas turbines but it is necessary to account for local flow conditions and development of boundary layers, when analysing hot surface ignition.

3.5.3 Initial temperature influence on the HSIT

It was experimentally shown by Mullen II et al. [1948] that increased initial temperature, decreases the HSIT. The same tendency are seen in the simulation results in Figure 3.13.

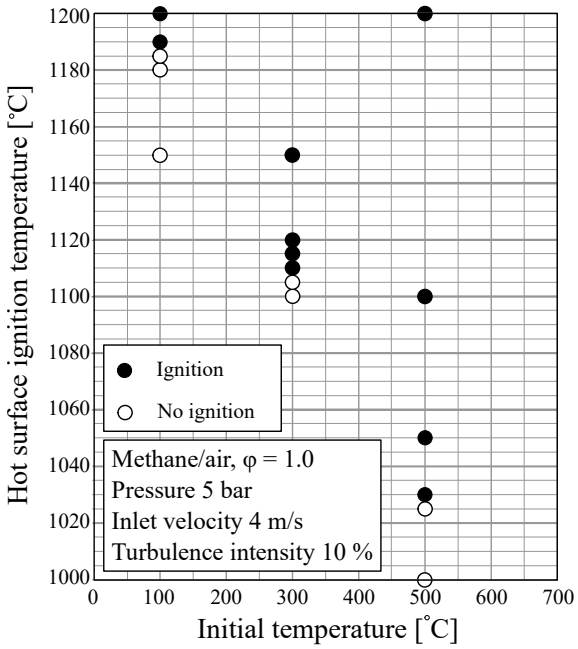

Figure 3.13. Simulation results illustrating the effect of changing the initial temperature on the HSIT.

As the initial temperature increases less energy needs to be transferred to the gas before achieving a gas temperature where ignition is a risk.

It is interesting to investigate the effect of initial temperature as the temperature increases as the gas is being compressed in the compressor section in the gas turbine. Typical compressor exit temperatures are in the range of 450-650°C with compression ratios of 17:1-35:1 under normal operation [Boyce, 2002]. Gas turbines on offshore facilities are often in the lower range of the compressibility ratios due to space and weight limitations on board [Lloyd's Register Consulting, 2016a]. Typical combustor liner and HP turbine surface temperatures of 1000°C would not ignite a flammable gas passing, under conditions simulated here.

Velocities at the compressor exit can be in the order of 150 m/s, completely rendering ignition impossible at normal operation. As the gas turbine is shutting down the compression ratio decreases, decreasing the initial gas temperature at the compressor exit. In order to determine the risk of ignition also the decreasing gas temperature should be taken into consideration.

3.5.4 Pressure influence on the HSIT

Found literature suggests that the the HSIT decreases with increased pressure. Similar to with increased initial temperature, increased pressure cause a more energy dense gas mixture, theoretically lowering the HSIT. Simulation results for changing pressure are presented in Figure 3.14.

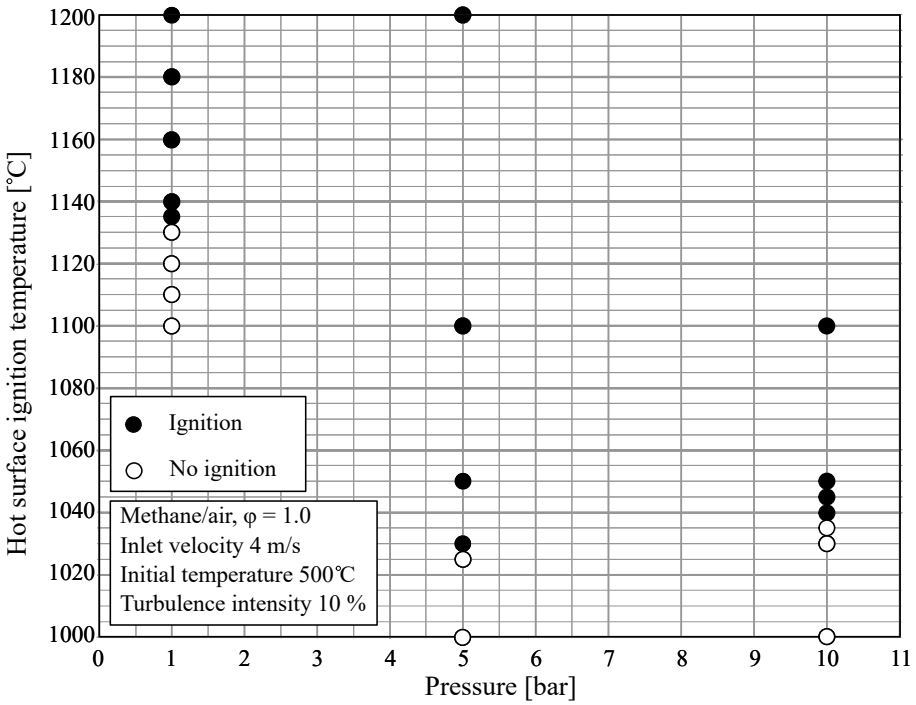

Figure 3.14. Simulation results illustrating the effect of changing the initial temperature on the HSIT.

Increasing the pressure from 1 to 5 bar follows the expected tendency with a decrease in HSIT. As the pressure increases to 10 bar the opposite behaviour is seen. As the pressure increases, so does the HSIT. It is true that chemically the risk of ignition increases with increased pressure. The activation energy decreases and the pre-exponential factor increases in addition to the ignition delay time decreases. This corresponds well with data showing that AIT decreases at elevated pressure. No data on pressure effect on HSIT is found in literature for pressure over 1.7 bar relative to vacuum. Hot surface ignition, compared to autoignition has a temperature gradient from the hot surface. The change in behaviour is due to the density increase with increasing pressure. As the pressure increases the density of the gas mixture increases causes the thermal diffusivity to drop. This causing the gas mixture to be less sensitive to temperature changes and increasing the minimum HSIT for ignition within same residence time. It is interesting how the dominant factor change in terms of the HSIT.

The effect on the HSIT of increasing the pressure is significant. From 1 to 5 bar pressure the HSIT drop by just above 100°C. The pressure range simulated here is low compared to what pressures are representative for gas turbines. As earlier presented compression ratios in the order of 17:1-35:1 are normal for industrial gas turbines [Boyce, 2002]. GE Oil and Gas' LM2500 and LM2500+ gas turbines, which are widely used in the Norwegian oil and gas industry, have a compression ratio of 18:1 and 23:1, respectively. Higher pressures should be investigated and preferable in relation to corresponding temperature and velocity shutdown profiles. Only with knowledge of the full coherence can the risk be better understood. One of the main reasons for the lower pressure range simulated is the applicability of the model, and mainly the empirical correlation for ignition delay time, validated from 0 to 10 atmospheric pressure.

3.6 Discussion of model applicability and sensitivity

Generally the model seems to predict physical behaviour well. Next step involves to run a sensitivity analysis on estimated expression and variables that could affect the results and therefore need to be chosen with care. Of examples can be mentioned the expression used to calculate the ignition delay time and the laminar flame speed. Both are used in a criterion of ignition and are expressed by a semi-empirical expression. The expression for the ignition delay time are purely valid for methane/air mixtures, so another expression should be found if the fuel or atmosphere are changed. The temperature range for which the ignition delay time are validated is only 1300-1900 K, which do not cover the entire temperature range that can be found in gas turbines, so it could be argued to find another expression or calculate an ignition delay based on detailed chemistry. Variables such as the activation energy, E_a, the pre-exponential factor, A, the overall reaction order, n, and the critical F-K parameter, δ_c are kept constant even though it is known that they change with temperature and pressure. With change of fuel and atmosphere the parameter change as well. Due to time restrictions a deeper analyses of how choices affect the simulation results are not done. It is recommended to do this before using the model further.

Another important step is to validate the model against experimental data to ensure trust in the specific HSITs. It could be done to validate against publicised experimental data if

contact to the authors were taken to get the missing information. Available experimental data on hot surface ignition are limited and in more so in terms of the effect of elevated pressures and turbulence. It is recommended to develop own experiments in case of further investigation of hot surface ignition.

The model takes starting point in already existing CFX models. This give rise to the model is limited to turbulent either premixed or partially premixed flow. The model are generally very flexible and else only limited if used expressions and variable values are defined for a specific range. With access to required CFX licenses these are easily changed so the model can be developed to apply to any geometry, fuel/atmosphere mixture, velocity, temperature, pressure and turbulence intensity. The model developed is merely on its initial state but showing potential.

4 Mitigation measures

With an estimated risk of ignition, that can lead to severe damage and loss of human life, it is relevant to look into practical solutions that can remove or limit the risk to an acceptable level.

Extensive historical use of mitigation measures to avoid hydrogen ignition in nuclear facilities results in an extensive knowledge pool. In nuclear facilities several mitigation techniques has been reported by IAEA [2011]. One way to remove hydrogen is to deliberately ignite the flammable gas so it burns with a slow deflagration, causing minimum damage. Another approach is venting. In an early stage of accidents, controlled venting is assumed to prevent total failure of the containment. The last mitigation measure reported by IAEA [2011] is inertisation of the containment atmosphere. Examples on candidates for inertisation are nitrogen and carbon dioxide. The effect on the flammability limits for hydrogen with added carbon dioxide and nitrogen are shown in Figure 4.1.

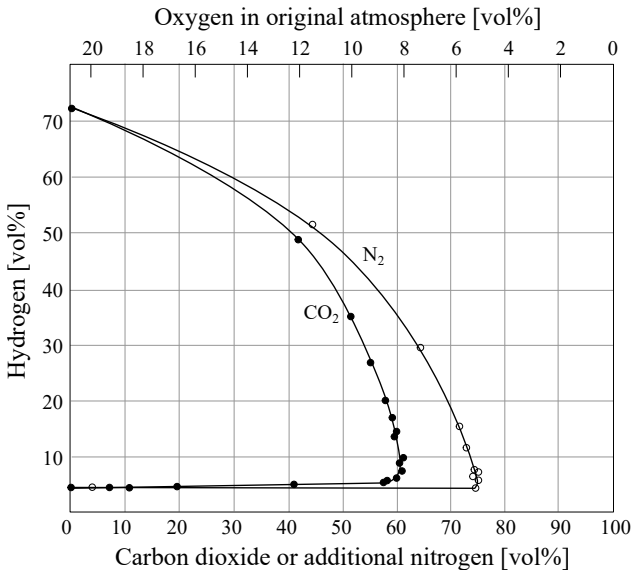

Figure 4.1. Flammability limit of hydrogen/air as a function of added carbon dioxide and nitrogen [Coward and Jones, 1952].

The general problem with carbon dioxide and nitrogen is that approximately 60 vol% and 75 vol%, respectively is needed to effectively dilute hydrogen in air [IAEA, 2011]. In practice diluting a flammable mixture is done by removing available oxygen so that the risk of combustion is nearly zero. For nitrogen this means that the oxygen level should be below 4.9 vol% in order to be non-flammable [Coward and Jones, 1952].

Some efforts were put into identifying interesting mitigation measures in the JIP Phase 0.

Cranking, or at times refereed to as windmilling, was proposed as an interesting solution [Lloyd's Register Consulting, 2016a]. Cranking the gas turbine has similar effect as venting in nuclear facilities. The increased velocity, lowers the residence time, lowering the risk of hot surface ignition. Removing the flammable gas is as well done faster, lowering the time with a potential risk of ignition. The flow profile though the gas turbine should be known in order to ensure no recirculation or stagnant zones are near a hot surface. This is quite a disadvantages with using cranking to mitigate. Another mitigation measure investigated was inertisation of the flammable gas, similar to what is done in nuclear facilities.

From preliminary investigation, inertisating the flammable gas with either water mist, inert gases or non-restricted halocarbons were found to be interesting to investigate further.

Water mist is an interesting diluent due to its favourable physical properties of evaporation. Water has a latent heat of vaporisation of 2,442 kJ/kg, and when it evaporates it expands 1700 times, drawing a lot of energy from the flammable gas and hinders access to oxygen [Stahl, 2004]. Disadvantages with the use of water mist to mitigate is the risk of accelerating fire instead of suppressing it. If too little water is added and the water molecule, H_2O, breaks down to OH radicals, the combustion reactions are aided instead of suppressed [Liu and Andrew, 1999].

Inert gas works purely by diluting the flammable mixture hindering access to oxygen. The large amounts of gas needed for diluting a flammable mixture with inert gases, such as nitrogen, was as well concluded in Phase 0 of the JIP. If diluting is only needed for a short duration it could still be relevant to use inert gas as a mitigation measure. Inerts are often easy to access and can be stored under high pressure [Lloyd's Register Consulting, 2016a].

Halocarbon is a chemical group where one or more carbon atoms are linked with one or more halogen atoms. Halogen atoms are the compounds found in group 17 of the periodic table e.g. fluorine, chlorine, bromine and iodine. The introduction of non-restricted halocarbons is interesting as smaller amounts are needed for diluting a flammable mixture. Halocarbons containing chlorine or bromine are, or will soon be, restricted due to the its negative effect on the ozone layer [UNEP Halons Technical Options Committee, 2014]. Halons containing bromine were in many years, the preferred measure for suppressing fire, due to its willingness to interact with important components of the combustion process. Halocarbons are at times referred to as chemical inhibitors or chemical active diluents.

Based on the concluded risk of ignition in Phase 0 of the JIP and the need for a practical solution, one of four main activities planned in Phase 1 of the JIP is: "*Feasibility studies of identified mitigation systems, and develop functional requirements to mitigation systems*" [Lloyd's Register Consulting, 2016b].

With inspiration from modelling the risk of mitigated hydrogen ignition in nuclear facilities the use of flammability limits as a requirement to mitigation systems is suggested.

4.1 Flammability limits as a requirement to mitigation systems

No ignition is possible outside the flammability limits. It is therefore a very practical criterion in risk analysis. In addition a lot of research has been conducted on the subject and, with a conservative safety factor, a set of requirements should be possible to develop relatively easy.

As mitigation measures are added to the flammable mixture, the range where the mixture is ignitable reduces. The effect on a methane/air mixtures flammability limits when adding different diluents are presented in Figure 4.2.

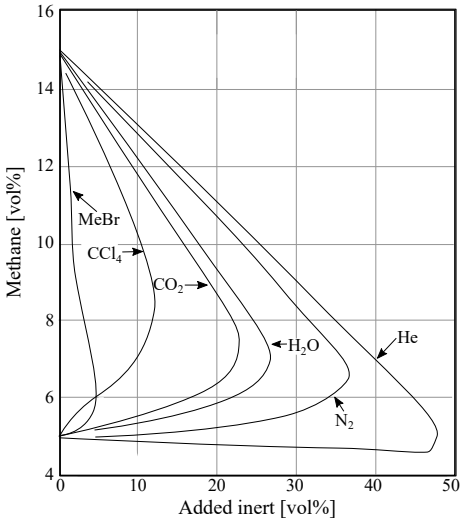

Figure 4.2. Flammability limit of methane/air as a function of added inert gases [Zabetakis, 1999]. Me is a methyl group, CH_3.

At atmospheric pressure and 25°C the minimum amounts of carbon dioxide and nitrogen to render a methane/air mixture non-flammable are 23 vol% and 37 vol%, respectively. Hydrocarbons with higher carbon index than methane and ethane can be represented in a generalized flammability diagram as they all require the same amount to extinguish a flame. Hydrocarbons with carbon index above 2 require 28 vol% and 42 vol% of carbon dioxide and nitrogen, respectively.

The use of semi-empirical correlations to determine the flammability limits has been presented earlier and used in the developed CFD model as a criterion for ignition. Methane was used in the developed CFD model, but a leak at an offshore facility would be natural gas (NG). The mixture composition of NG change based on place of origin. The LFL of NG, and any mixture of paraffin hydrocarbons, can be calculated by Le Chatelier's law in Equation (4.1) [Coward and Jones, 1952] [Zabetakis, 1999].

$$\mathrm{LFL} = 100/\left(\sum_{i=1}^{n}\frac{C_i}{\mathrm{LFL}_i}\right), \qquad \sum_{i=1}^{n} C_i = 100 \tag{4.1}$$

where:			
	C	Percentage composition	[%]
	LFL	Lower Flammability Limit	[vol%]
	n	Number of species	[–]

The law is as well valid for other atmospheres then air, e.g. methane in a wide range of oxygen-nitrogen mixtures and in air-carbon dioxide, air-argon and air-helium. In addition the law is valid for hydrogen and carbon monoxide in mixtures of air, nitrogen and carbon dioxide [Coward and Jones, 1952]. To use Le Chatelier's law with diluents a small recalculation is required to determine the "air-free" mixture composition. For more details on the procedure please refer to Coward and Jones [1952].

Kondo et al. [2006] developed a semi-empirical extension to Le Chatelier's expression for both the LFL and UFL for a range of fuel/air mixtures diluted with nitrogen. It was later found that the same expressions were true for diluting with carbon dioxide [Kondo et al., 2009]. The expression for LFL and UFL are shown in Equation (4.2) and (4.3), respectively.

$$\frac{C_1}{\mathrm{LFL}_{mix}} = \frac{C_1}{\mathrm{LFL}_1} + pC_{in} \tag{4.2}$$

$$\frac{C_1 n_1}{100 - (\mathrm{UFL}_{mix}/C_1)} = \frac{C_1 n_1}{100 - \mathrm{UFL}_1} + qC_{in} + rC_{in}^2 + sC_{in}^3 \tag{4.3}$$

where:			
	C_{in}	Fraction of inert gas, $C_{in} = 1 - C_1$	[%]
	p, q, r, s	Parameters to be determined experimentally	[–]

Subscript meaning:

mix	Total fuel, air and inert gas mixture limit	[–]
1	Reference to the fuel/air on its own	[–]

Where n_1 is determined by Equation (4.4).

$$n_1 = \frac{0.21(100 - \mathrm{UFL}_1)}{\mathrm{UFL}_1} \tag{4.4}$$

Kondo et al. [2006] found that the same parameter values could be used for methane, propane, propylene, methyl formate and 1,1-Difluoroethane diluted with either nitrogen or carbon dioxide. The parameter values are shown in Table 4.1.

p	q	r	s
-0.00187	0.00122	0.00187	-0.00242

Table 4.1. Experimentally determined parameter values to determine the LFL and UFL for methane, propane, propylene, methyl formate and 1,1-Difluoroethane diluted with nitrogen and carbon dioxide as of Equation (4.2) and (4.3) [Kondo et al., 2006]

Kondo et al. [2009] showed that flammability limits when diluting with HFC-125, a widely used non-restricted halocarbon with the formula CF_3CHF_2, could as well be described by semi-empirical expressions. To calculate the LFL a parameter times C_{in} to the second and third power are added. Kondo et al. [2009] also found that no common parameter values were possible for different fuels. The reason for extra complexity is that HFC-125 is involved in the chemical reactions and is not a pure inert as is the case for nitrogen

and carbon dioxide [Kondo et al., 2009]. The more sophisticated suppression effects from halocarbons makes it more complicated to calculate.

Determining the flammability limits in complex mixtures are often determined experimentally through standardised tests [Shebeko et al., 2002]. Attempts to determine flammability limits analytically are often based on empirical data, such as done by Kondo et al. [2009]. Shebeko et al. [2002] developed an analytic approach to determine the flammability limits with added diluent of both the inert and chemical active category. The method is developed based on an understanding of the important chain reactions, hereunder the formation of the CO, and that flammability limits of various diluted mixtures follow the typical curve illustrated in Figure 4.3.

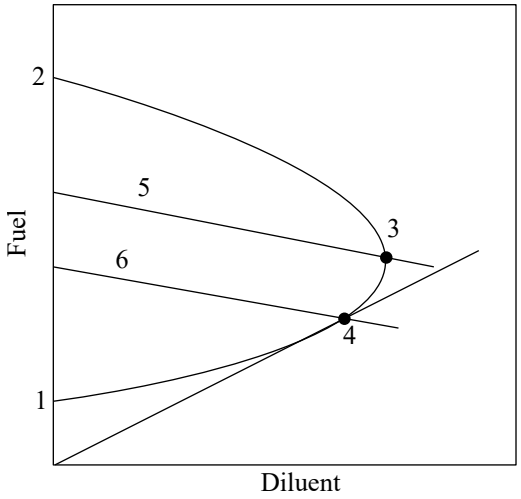

Figure 4.3. Typical flammability curve. 1: LFL, 2: UFL, 3: Inertisation peak point, 4: The mixture limiting on flammability, 5: Line of mixture stoichiometric in relation to combustion up to CO and H_2O and 6: Line of mixture stoichiometric in relation to combustion up to CO_2 and H_2O [Shebeko et al., 2002].

In order to analytically determine the flammability limits, expressions for the LFL, line 1 in Figure 4.3, UFL, line 2 in Figure 4.3, inertisation peak point, point 3 in Figure 4.3, and the mixture limiting on flammability, point 4 in Figure 4.3, are derived whereby the full flammability curve is described. For the LFL, the inertisation peak point and the mixture limiting on flammability point a conservation of energy equation forms the basis for the derived model. Due to the complex kinetics at the UFL an empiric equation is used for that estimation [Shebeko et al., 2002].

The main parameters required to evaluate the flammability curve are the adiabatic flame temperature and the effective equivalence ratio related to burning up CO and H_2O. For details on the derivation of each expression please refer to Shebeko et al. [2002]. In the study calculations were made on 75 mixtures of various art. 49 of the mixtures were with inert diluents and the remaining 26 were with chemical active halocarbon diluents. A root mean square (RMS) error of 12.5% and 11.3% on the LFL for inert and chemical active diluents was calculated when comparing to experimental data. For the UFL RMS errors of 16.0% and 12.9% were calculated for inert and chemical active diluents [Shebeko et al., 2002].

Liao et al. [2005] compared experimental data on flammability limits with calculated limits by the method of Shebeko et al. [2002] on NG in air diluted with nitrogen and carbon dioxide. The result can be seen in Figure 4.4.

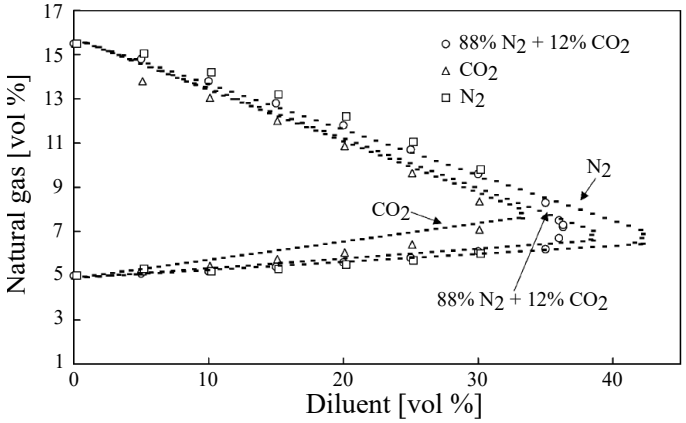

Figure 4.4. Experimental and calculated flammability limits of natural gas in air diluted with nitrogen and/or carbon dioxide [Liao et al., 2005].

It is very relevant to be aware of that the model by Shebeko et al. [2002] seems to under predict the flammable range if using the model in risk analysis. As the procedure by Shebeko et al. [2002] is based on energy conservation and thereby adiabatic flame and initial temperatures it could be estimated that the model could be used at increased temperatures, as investigated in this thesis. Increased pressures could potentially also be accounted for when determining the physical parameter values forming the basis for modelling. No papers or other publications of this are found, leaving an area of research that with great interest could be investigated further.

As the pressure and initial temperature increase, so does the flammable range and the amount of diluent needed to extinguish a flame [Zabetakis, 1999]. Figure 4.5 shows how the flammability limits are affected with increased pressure for a NG/air mixture diluted with nitrogen.

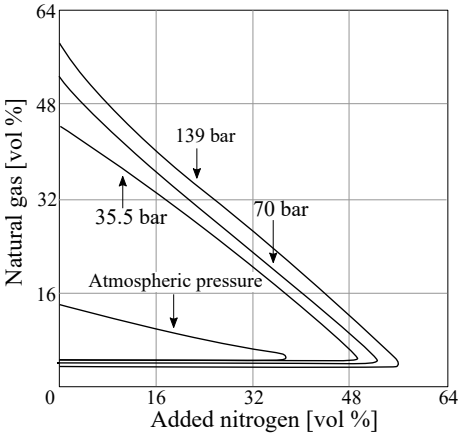

Figure 4.5. Flammability limits of natural gas/air mixture diluted with nitrogen [Zabetakis, 1999].

This section focused on modelling procedures for determining flammability limits with diluents. Extensive experimental data is available in the literature. In case it is decided to utilise flammability limits as a requirement to mitigation systems, further literature survey is recommended. Additional information on modelling procedures at elevated pressure and temperature could as well be relevant to find or develop before using flammability limits as a requirement.

A suggestion on how mitigation measures can be included in the developed CFD model is presented next.

4.2 Including mitigation measures in the developed CFD model

Implementation of flammability limits with diluents can be done in the same way as with the flammability limits that are expressed as a function of temperature and pressure implemented in the developed CFD model.

It is necessary to include the effective change in mixture composition that mitigation measures cause as well. Including water, nitrogen and carbon dioxide diluents in the developed CFD model can be done in the step where the flamelet library is generated. In the CFX-RIF tool, that generate the flamelet libraries, several options are available. There are built in reaction mechanisms of hydrogen, methane, propane, heptane, carbon oxide/hydrogen mixtures, methane/hydrogen mixtures, C1-C4 mixtures and gasoline (octane/heptane). Additional mechanisms for diesel and Jet-A are included with use of surrogate fuels. It is an option to define the mass fraction of each species, making it possible to also model e.g. natural gas with the C1-C4 reaction mechanism. Under the oxidiser, compositions mass fractions of carbon dioxide, water, oxygen and nitrogen can be assigned, making it possible to model other atmospheres than air.

The boundary temperature of fuel and oxidiser can be assigned different values. In addition the BVM with the flamelet sub-model are developed for premixed or partially premixed combustion, so for a geometry with several inlets different mixing and cooling effects can also be included in the model.

It is at this point in time not possible to include the halocarbon diluents in the demonstration model. In order to include the chemical active diluents the reaction mechanism should be determined and included in the form readable by CFX-RIF. Inspiration for the task can be found in the .ccl and .dat files for the existing mechanisms which can be found under *Program Files* → *ANSYS Inc* → *vXXX* → *CFX* → *etc* → *cfxrif*, where the *vXXX* is dependent on the ANSYS version installed. Notice that the CFX-RIF requires a separate license in order to generate the flamelet libraries.

5 Conclusion

Ignition and combustion characteristics of flammable gas mixture passing over hot surfaces are investigated through three main activities.

The first activity was to conduct an extensive literature survey in order to gain an understanding of ignition and combustion characteristics over hot surfaces and in addition determine state of the art within this subject. The literature survey is important as it forms the basis for the rest of the study. It is found that the complex nature of hot surface ignition and combustion leads to a relatively sparse pool of knowledge on the subject. The main contributors to the fundamental understanding of minimum hot surface temperature leading to ignition, and how physical and chemical parameters affect that temperature, are the experimental studies by Mullen II et al. [1948] and Smyth and Bryner [1991]. It is similarly found that only few studies are available that try to model hot surface ignition and combustion. No academic, industrial or commercial available codes covers both ignition and combustion characteristics of flammable gas ignition due to hot surfaces. Two studies modelling the ignition initiation are found where none include the combustion characteristics. Commercial risk analysis codes modelling combustion are all found to be manually ignited based on a "worst case" scenario. Inspiration to a modelling procedure was found in this literature study by including elements from each.

Development and implementation of a working model in ANSYS CFX has been successful. In order to model combustion the BVM with the laminar flamelet sub-model is used. The advantages of these models include the introduction of the reaction progress variable. All chemical kinetics are handled through this parameter, making it computationally easier to handle. Determination of ignition time and position is done by investigating where the reaction progress variable first has a value above zero. A set of criteria are set up so no ignition is initiated unless they are fulfilled.

The model behaves in accordance with expected tendencies found in the literature study. As the inlet velocity increases, the residence time decreases, and the HSIT increases. The model can be used to estimate the risk of ignition under a set of physical conditions. It can for example be estimated that with surface temperatures inside the gas turbine in the proximity of 1000°C the velocity should be minimum 4 m/s in order to avoid ignition. This estimation is based on methane/air under stoichiometric conditions, 5 bar pressure, an initial temperature of 500°C and a turbulence intensity of 10%.

It is estimated very unlikely for a flammable mixture to ignite in gas turbines under operation as velocities are far above 4 m/s. Simulations conclude that increasing initial temperature, causes the HSIT to decrease. This is in coherence with the tendency experimentally observed by Mullen II et al. [1948]. The effect of increased inlet velocity and

increased initial temperature are well documented in literature to increase and decrease the HSIT, respectively.

Less information are available in terms of the effects from turbulence and increased pressure on the HSIT. Simulation results show that the HSIT increases with increased turbulence. Mullen II et al. [1948] estimate the same behaviour without measuring it directly. Flow in gas turbines are subject to high turbulence, which can work as an ignition inhibitor due to mixing the cold flow with the hot flow near the wall, rendering ignition more difficult.

It was observed that the HSIT decreases with increasing pressure in a range of 1-1.7 bar [Mullen II et al., 1948]. Generally very little information is available on higher pressures, both in terms of flammability limits and hot surface ignition. Gas turbines operate at very high pressure ranges and pressure is therefore a very important parameter to understand the effect from. An interesting tendency was observed in the simulation results as the pressure was increased from 5 bar to 10 bar. Instead of decreasing, the HSIT increased by 5°C. The reason for this are the increased density with increased pressure. As the density increases the thermal diffusivity decreases resulting in a flow that is less sensitive to changes in temperature and therefore is slower in heating up to a state where ignition is possible.

Based upon understanding the hot surface ignition and combustion characteristics the last activity of the thesis is to investigate mitigation measures that can effectively suppress fire and explosions in gas turbines on offshore facilities. Inspiration on mitigation measures is collected for mitigating hydrogen ignition in nuclear facilities. In nuclear facilities mitigation measures include controlled combustion, venting and inertisation of the flammable atmosphere. Controlled combustion is less attractive in the gas turbine due to the complex geometry and already stressed material. The risk of losing control and inducing a serious risk of damage to the gas turbine is unacceptable. Venting can be done by cranking, also at times referred to as windmilling, the gas turbine. Cranking ensure a flow trough the gas turbine keeping the velocity up. It was seen from the simulation result that the increased velocities lower the risk of hot surface ignition. With the use of cranking the flow profile should be known in order to ensure no recirculation or stagnant flow zones being near a hot surface introducing a risk of ignition. Inertisation of the flammable atmosphere is an option in the gas turbine as well. With added diluents the flammable range decreases and if enough is added the gas can be rendered non-flammable. A very functional requirement to mitigation systems are the flammability limits, also used as a criterion for mitigation measures in nuclear facilities. Unlike hot surface ignition quite an extensive literature pool exists on flammability limits and the effect of added diluents. Flammability limits are a practical requirement to a mitigation system, as it does not require a detailed 3D modelling of a gas turbine in order to know the specific flow profile. With a conservative safety factor and ensuring a somewhat uniform mixing of flammable gas and diluent, the risk of ignition can be limited to an acceptable level with less effort then required to develop a detailed CFD model. Note that it requires an extra investment of a system of injection nozzles and diluent storage. By comparison, cranking requires no extra investments.

Bibliography

American Petroleum Institude, **2003**. American Petroleum Institude. *Ignition Risk of Hydrocarbon Liquids and Vapors by Hot Surfaces in the Open Air*. API Recommended Practice 2216m, Third Edition, 2003.

ANSYS, Inc., **2009**. ANSYS, Inc. *Introduction to CFX. Chapter 8, Transient Simulations*. URL: `www.racfd.com/cfx/CFX12_08_Transient.ppt`, 2009. Acquired: 26-05-2016.

ANSYS, Inc, **2016**. ANSYS, Inc. *ANSYS CFX-Solver Theory Guide*. ANSYS CFX Release 17, 2016.

Bielert, Breitung, Kotchourko, Royl, Scholtyssek, Veser, Beccantini, Dabbene, Paillere, Studer, Huld, Wilkening, Edlinger, Poruba, and Mohaved, **2001**. U. Bielert, W. Breitung, A. Kotchourko, P. Royl, W. Scholtyssek, A. Veser, A. Beccantini, F. Dabbene, H. Paillere, E. Studer, T. Huld, H. Wilkening, B. Edlinger, C. Poruba, and M. Mohaved. *Multidimensional Simulatin of Hydrogen Distribution and Turbulent Combustion in Severe Accidents*. Nuclear Engineering and Design, 209, 165–172, 2001.

Boettcher, **2012**. Philipp Andreas Boettcher. *Thermal Ignition*. Ph.D thesis, California Institude of Technology, 2012.

Bounaceur, Glaude, Sirjean, Fournet, Montagne, Vierling, and Moliére, **2015**. Roda Bounaceur, Pierre-Alexandre Glaude, Baptiste Sirjean, René Fournet, Pierre Montagne, Matthieu Vierling, and Michel Moliére. *Prediction of auto-ignition temperatures and delays for gas turbine applications*. Proceedings of ASME Turbo Expo 2015: Turbine Technical Conference and Exposition, 2015.

Boyce, **2011**. Meherwan P. Boyce. *Gas Turbine Engineering Handbook*. ISBN: 978-0-12-383842-1. Elsevier, 2011.

Boyce, **2002**. Meherwan P. Boyce. *Gas Turbine Engineering Handbook*. ISBN: 0-88415-732-6. Butterworth-Heinemann, 2002.

Bradley, **1996**. Derek Bradley. *'Hot spots' and gasoline engine knock*. Journal of the Chemical Society, Faraday Transaction, 92, 2959–2964, 1996.

Cant and Mastorakos, **2008**. R. S. Cant and E Mastorakos. *An Introduction to Turbulent Reacting Flows*. ISBN: 978-1-86094-778-0. Imperial College Press, 2008.

Caron, Goerhals, Smedt, Berghmans, Vliegen, Oost, and Aarssen, **1999**. M. Caron, M. Goerhals, G. De Smedt, J. Berghmans, S. Vliegen, E. Van't Oost, and A van den Aarssen. *Pressure dependence of the auto-ignition temperature of methane/air mixtures.* Journal of Hazardous Materials, 65, Issue 3, 233–244, 1999.

Cashdollar, Zlochower, Green, Thomas, and Hertzberg, **2000**. Kenneth L. Cashdollar, Isaac A. Zlochower, Gregory M. Green, Richard A. Thomas, and Martin Hertzberg. *Flammability of methane, propane, and hydrogen gases.* Jornal of Loss Precention in the Process Industries, 13, 327–340, 2000.

Cassel and Liebman, **1963**. H. M. Cassel and I. Liebman. *Combustion of magnesium particles II-Ignition temperatures and thermal conductivities of ambient atmospheres.* Combustion and Flame, 7, 79–81, 1963.

Chillé, Bakke, and Wingerden, **2008**. F. Chillé, J. R. Bakke, and K. van Wingerden. *Use of CFD tools for prediction of explosion loads.* Handling Exceptions in Structural Engineering, Rome, 2008.

Colwell and Reza, **2005**. Jeff D. Colwell and Ali Reza. *Hot Surface Ignition of Automotive and Aviation Fluids.* Fire Technology, 41, 105–123, 2005.

Coward and Jones, **1952**. H. F. Coward and G. W. Jones. *Limits of Flammability of Gases and Vapors.* Bureau of Mines, Bulletin 503, 1952.

Det Norske Veritas, **2007**. Det Norske Veritas. *Accident statistics for floating offshore units on the UK Continental Shelf 1980-2005.* Prepared for Health and Safety Executive (HSE), Research Report RR567, 2007.

Fire Protection Association, **2014**. Fire Protection Association. *Fire Safety and Risk Management.* ISBN: 978-0-415-81731-8. Routledge, 2014.

Fontanesi, Paltrinieri, D'Adamo, Cantore, and Rutland, **2013**. Stefano Fontanesi, Stefano Paltrinieri, Alessandro D'Adamo, Giuseppe Cantore, and Christopher Rutland. *Knock Tendency Prediction in a High Performance Engine Using LES and Tabulated Chemistry.* SAE Int. J. Fuels Lubr., 6, 98–118, 2013.

Fontanesi, Cicalese, D'Adamo, and Cantore, **2014**. Stefano Fontanesi, Giuseppe Cicalese, Alessandro D'Adamo, and Giuseppe Cantore. *A methodology to improve knock tendency prediction in high performance engines.* Energy Procidia, 45, 769–778, 2014.

Galarça and França, **2007**. Marcelo M. Galarça and Francis H. R. França. *Correlations for Radiative Nusselt Number for Combined Convective and Thermal Radiation Heat Transfer in Smoketube Steam Generators.* 19th International Congress of Mechanical Engineering, Proceedings of COBEM, 2007.

GE Oil & Gas, **2016**. *GE Oil & Gas.* JIP meeting, January, 2016.

HSE - Offshore Division, **2013**. HSE - Offshore Division. *Fire and Explosion Strategy - Issue 1.* URL: `http://www.hse.gov.uk/offshore/strategy/index.htm`, 2013. Acquired: 04-04-2016.

Hu, Li, Meng, Chen, Cheng, Xie, and Huang, **2015**. Erjiang Hu, Xiaotian Li, Xin Meng, Yizhen Chen, Yu Cheng, Yongliang Xie, and Zuohua Huang. *Laminar flame speeds and ignition delay times of methane-air mixtures at elevated temperatures and pressures.* FUEL, 158, 1–10, 2015.

IAEA, **2011**. International Atomic Energy Agency IAEA. *Mitigation of Hydrogen Hazards in Severe Accidents in Nuclear Power Plants.* TECDOC-1661, Vienna, 2011.

Kalghatgi and Bradley, **2012**. Gautam T Kalghatgi and Derek Bradley. *Pre-ignition and 'super-knock' in turbo-charged spark-ignition engines.* International Journal of Engine Research, 13, 399–414, 2012.

Kondo, Takizawa, Takahashi, and Tokuhasho, **2006**. Shigeo Kondo, Kenji Takizawa, Akifumi Takahashi, and Kazuaki Tokuhasho. *Extended Le Chatelier's formula and nitrogen dilution effect on the flammability limits.* Fire Safety Journal, 41, 406–417, 2006.

Kondo, Takizawa, Takahashi, Tokuhasho, and Sekiya, **2009**. Shigeo Kondo, Kenji Takizawa, Akifumi Takahashi, Kazuaki Tokuhasho, and Akira Sekiya. *Flammability limits of five selected compounds each mixed with HFC-125.* Fire Safety Journal, 44, 192–197, 2009.

Kondo, Takizawa, Takahashi, and Tokuhasho, **2011**. Shigeo Kondo, Kenji Takizawa, Akifumi Takahashi, and Kazuaki Tokuhasho. *On the temperature dependence of flammability limits of gases.* Journal of Hazardous Materials, 187, 585–590, 2011.

Kong, Eckhaff, and Alfert, **1994**. Dehong Kong, Rolf K. Eckhaff, and Franz Alfert. *Auto-ignition of CH_4/air, C_3H_8/air, CH_4/C_3H_8/air, CH_4/CO_2/air using a 11 ignition bomb.* Journal of Hazardous Materials, 40, 69–84, 1994. (University of Bergen, Christian Michelsen Research AS).

Laurendeau, **1982**. Normand M. Laurendeau. *Thermal Ignition of Methane-Air Mixtures by Hot Surfaces: A Critical Examination.* Combustion and Flame, 46, 29–49, 1982.

Lea and Ledin, **2002**. C. J. Lea and H. S. Ledin. *A Review of the State-of-the-Art in Gas Explosion Modelling.* Health and Safety Laboratory (HSL), Fire and Explosion Group, 2002.

Lees, **2012**. Frank Lees. *Lees' Loss Prevention in the Process Industries - Hazard Identification, Assessment and Control.* ISBN: 978-0-12-397210-1. Elsevier, 2012.

Liao, Cheng, Jiang, and Gao, **2005**. S.Y. Liao, Q. Cheng, D.M. Jiang, and J. Gao. *Experimental study of flammability limits of natural gas-air mixture.* Journal of Hazardous materials, B119, 81–84, 2005.

Linse, Kleemann, and Hasse, **2014**. Dirk Linse, Andrean Kleemann, and Christian Hasse. *Probability density function approach coupled with detained chemical kinetics for the prediction of knock in turbocharged direct injection spark ignition engines.* Combustion and Flame, 161, 997–1014, 2014.

Liu and Andrew, **1999**. Zhigang Liu and K. Kim Andrew. *A review of water mist fire suppression systems-fundamental studies.* Journal of fire protection engineering, 10.3, 32–50, 1999.

Lloyd's Register Consulting, **2015**. Lloyd's Register Consulting. *JIP gas turbine intake system - Detailed Scoping Phase.* Internal LRC document: Confidential, for restricted circulation only, 2015.

Lloyd's Register Consulting, **2016a**. Lloyd's Register Consulting. *Preliminary Investigation of Gas Turbines as an Ignition Source and Potential Mitigation Measures.* Technical note - 1. Internal JIP document: Distribute only after client's acceptance, 2016.

Lloyd's Register Consulting, **2016b**. Lloyd's Register Consulting. *Gas turbine air intake ignition control - Phase 0, Joint Industry Project.* Report-1. Internal JIP document: Distribute only after client's acceptance, 2016.

Lloyd's Regiter Consulting, **2015**. *Lloyd's Regiter Consulting.* Internal JIP meeting, 2015.

Markides, **2016**. Christos N. Markides. *Autoignition in Turbulent flows.* URL: `http://www2.eng.cam.ac.uk/~cnm24/autoignition.htm`, 2016. Acquired: 17-02-2016.

Mullen II, Fenn, and Irby, **1948**. James W. Mullen II, John B. Fenn, and Moreland R. Irby. *The Ignition of High Velocity Streams of Combustible Gases by Heated Rods.* Third Symposium on Combustion and Flame and Explosion Phenomena, 3, 317–329, 1948.

Paik, Czujko, Kim, Seo, Ryu, Ha, Janiszewski, and Musial, **2011**. Jeom Kee Paik, Jerzy Czujko, Bong Ju Kim, Jung Kwan Seo, Han Seong Ryu, Yeon Chul Ha, Piotr Janiszewski, and Beata Musial. *Quantitative assessment of hydrocarbon explosion and fire risks in offshore installations.* Marine Structures, 24, 73–96, 2011.

Pedersen, **2005**. Aleksander Pedersen. *Ignition probability of a flammable mixture exposed to a gas turbine.* Master's Thesis, Environmental engineering, Norwegian Institute of Science and Technology, 2005.

PSA, Norway, **2016**. PSA, Norway. *Hydrocarbon leaks have a major accident potential, highlighted by the destruction of the Piper Alpha platform on the UK continental shelf in 1988, when 167 lives were lost.* URL: `http://www.psa.no/process-integrity/hydrocarbon-leaks-and-fires-article4162-902.html`, 2016. Acquired: 17-02-2016.

Rasmussen and Sødring, **2008**. Niels Bjarne K. Rasmussen and Thomas W. Sødring. *The Ignition Parameter - A quantification of the probability of ignition.* European Conference on Industrial Furnaces and Boilers (INFUB), 2008.

Shebeko, Fan, Bolodian, and Navzenya, **2002**. Yu. N. Shebeko, W. Fan, I. A. Bolodian, and V. Yu Navzenya. *An analytical evaluation of flammability limits of*

gaseous mixtures of combustible-oxidizer-diluent. Fire Safety Journal, 37, 549–568, 2002.

Sherman and Bergen, **1987**. M. P. Sherman and M. Bergen. *The Possibility of Local Detonations During Degraded-Core Accidents in the Bellefonte Nuclear Power Plant.* For the United States Department of Energy, California, 1987.

Sherman and Bergen, **2005**. M. P. Sherman and M. Bergen. *Analysis methodology for hydrogen behaviour in accident scenarios.* International Conference on Hydrogen Safety, Pisa, 2005.

Smyth and Bryner, **1991**. K. C. Smyth and N. P. Bryner. *Short-duration Autoignition Temperature Measurements for Hydrocarbon Fuels.* National Institute of Standard and Technology (NIST), 1991.

Stahl, **2004**. D. P. Stahl. *A Thermodynamic examination og the extinguidhing properties of water spray and water mist.* 6th Asia-Oceania Symposium on Fire Science and Technology, 2004.

Takeno, **1977**. Tadao Takeno. *Ignition Criterion by Thermal Explosion Theory.* Combustion and Flame, 29, 209–211, 1977.

The Guardian, **2013**. The Guardian. *Piper Alpha disaster: how 167 oil rig workers died.* URL: `http://www.theguardian.com/business/2013/jul/04/piper-alpha-disaster-167-oil-rig`, 2013. Acquired: 17-02-2016.

UNEP Halons Technical Options Committee, **2014**. UNEP Halons Technical Options Committee. *Fire Protection Alternatives to Halons.* Montreal Protocol on Substances that Deplete the Ozone Layer, Technical Note #1 - Revision 4, 2014.

Üngüt, **2001**. A. Üngüt. *CFD simulation and detailed chemical modelling of alkane autoignition near a heated metal surface.* Shell Global Solutions (UK) Contract research report 35 for Health and Safety Executive (HSE), 2001.

Vancoillie, Demuynck, Galle, Verhelst, and Oijen, **2012**. Jeroen Vancoillie, Joachim Demuynck, Jonas Galle, Sebastian Verhelst, and J. A. van Oijen. *A laminar burning velocity and flame thickness correlation for ethanol-air mixtures valid at spark-ignition engine conditions.* FUEL, 102, 460–469, 2012.

Vanderstraeten, Tuerlinckx, Berghmans, Vliegen, Oost, and Smit, **1997**. B. Vanderstraeten, D. Tuerlinckx, J. Berghmans, S. Vliegen, E. Van't Oost, and B. Smit. *Experimental study of the pressure and temperature dependence on the upper flammability limit of methane/air mixtures.* Journal of Hazardous Materials, 56, 237–246, 1997.

Versteeg and Malalasekera, **2007**. H. K. Versteeg and W. Malalasekera. *An Introduction to Computational Fluid Dynamics - The Finite Volume Method.* ISBN: 978-0-13-127498-3. Pearson Education Limited, 2007.

Vinnem, **2014**. Jan-Erik Vinnem. *Offshore Risk Assessment Vol 1 - Principals, Modelling and Applications of QRA Studies.* ISBN: 978-1-4471-5206-4. Springer, 2014.

Vlahostergiosa, Missirlisa, Flourosb, Albanakisa, and Yakinthosa, **2015**. Z. Vlahostergiosa, D. Missirlisa, M. Flourosb, C. Albanakisa, and K. Yakinthosa. *Effect of turbulence intensity on the pressure drop and heat transfer in a staggered tube bundle heat exchanger.* Experimental Thermal and Fluid Science, 60, 75–82, 2015.

White, **1925**. Albert Greville White. *XCVI.- Limits for the propagation of flame in inflammable gas-air mixtures. Part III. The effects of temperature on the limits.* J. Chem. Soc., Trans., 127, 672–684, 1925.

Zabetakis, **1999**. Michael G. Zabetakis. *Flammability characteristics of combustible gases and vapors.* U.S. Bureau of Mines, Bulletin 627, 1999.

Zaccardi, Duval, and Pagot, **2009**. Jean-Marc Zaccardi, Laurent Duval, and Alexandre Pagot. *Development of specific tools for analyis and quantification of pre-ignition in a boosted SI engine.* SAE International paper 01-1795, 2009.

Zeldovich, Barenblatt, Librovich, and Makhviladze, **1985**. Ya. B. Zeldovich, G. I. Barenblatt, V. B. Librovich, and G. M. Makhviladze. *The mathematical theory of combustion and explosions.* Consultants Bureau, Plenum Press, New York, 1985.

A Overview of CFX settings for simulation

The settings used for the simulations in CFX are listed in Table 3.1.

Run Definition		
Type	Transient	
Options	Double Precision	
	Large Problem	
Run model	Parallel, Partitions 2	
Solver Control - Basic Settings		
Advection Scheme	High Resolution	
Transient Scheme	Second Order Backward Euler	
	Automatic time step initialisation	
Turbulence numerics	First Order	
Convergence control	Min. Coefficient Loops = 1	
	Max. Coefficient Loops = 5	
Convergence criteria	RMS 1e-4	
Materials		
Material definition	Reacting Mixture	
Components	CH	H2O
	CH2O	H2O2
	CH3	HO2
	CH4	N2
	CHO	O
	CO	O2
	CO2	OH
	H	x3 CH2
	H2	

Table A.1. Simulation settings in CFX.

B Simulation results

Simulations are conducted where inlet velocity, turbulence intensity, initial temperature and pressure are changed in order to investigate the effect on HSIT. Simulation results for the basic case are presented in Table B.1.

Surface temp.	Ign. time [s]	Ign. position
915	— No ignition —	
950	— No ignition —	
1000	— No ignition —	
1025	— No ignition —	
1030	0.25	z = 0.5
1050	0.19	z = 0.35
1100	0.12	z = 0.1
1200	0.07	z = 0.0
1500	0.06	z = 0.0

Table B.1. Simulation results with inlet velocity = 4 m/s, Turbulence intensity = 10 %, Initial temperature = 500°C and Pressure = 5 bar.

B.1 Inlet velocity influence on the HSIT

Surface temp.	Ign. time [s]	Ign. position
600	— No ignition —	
650	— No ignition —	
670	— No ignition —	
675	6.64	z = 0.49
680	5.71	z = 0.48
700	4.06	z = 0.29
900	1.03	z = 0.0

Table B.2. Simulation results with inlet velocity = 0.2 m/s.

Surface temp.	Ign. time [s]	Ign. position
800	— No ignition —	
900	— No ignition —	
910	— No ignition —	
915	0.53	z = 0.5
920	0.48	z = 0.4
950	0.31	z = x.x
1000	0.18	z = x.x
1200	0.11	z = x.x

Table B.3. Simulation results with inlet velocity = 2 m/s.

Surface temp.	Ign. time [s]	Ign. position
1100	— No ignition —	
1200	— No ignition —	
1215	— No ignition —	
1220	0.11	z = 0.5
1225	0.1	z = 0.5
1230	0.1	z = 0.5
1245	0.09	z = 0.46
1245	0.09	z = 0.45
1300	0.07	z = 0.3
1600	0.03	z = 0.04
2000	0.02	z = 0.0

Table B.4. Simulation results with inlet velocity = 10 m/s.

B.2 Turbulence intensity influence on the HSIT

Surface temp.	Ign. time [s]	Ign. position
995	— No ignition —	
1000	0.26	z = 0.49
1030	0.1	z = 0.05

Table B.5. Simulation results with turbulence intensity = 1 %.

Surface temp.	Ign. time [s]	Ign. position
995	— No ignition —	
1000	0.27	z = 0.5
1005	0.25	z = 0.45
1010	0.23	z = 0.4
1015	0.21	z = 0.4

Table B.6. Simulation results with turbulence intensity = 5 %.

B.3 Initial temperature influence on the HSIT

Surface temp.	Ign. time [s]	Ign. position
1150	— No ignition —	
1180	— No ignition —	
1185	0.23	z = 0.5
1190	0.21	z = 0.45
1200	0.19	z = 0.4

Table B.7. Simulation results with initial temperature = 100°C.

Surface temp.	Ign. time [s]	Ign. position
1100	— No ignition —	
1105	— No ignition —	
1110	0.25	z = 0.5
1115	0.23	z = 0.5
1120	0.21	z = 0.44
1150	0.15	z = 0.25

Table B.8. Simulation results with initial temperature = 300°C.

B.4 Pressure influence on the HSIT

Surface temp.	Ign. time [s]	Ign. position
1100	— No ignition —	
1110	— No ignition —	
1120	— No ignition —	
1130	— No ignition —	
1135	0.13	z = 0.08
1140	0.12	z = 0.08
1160	0.1	z = 0.08
1180	0.08	z = 0.05
1200	0.07	z = 0.04

Table B.9. Simulation results with pressure = 1 bar.